Electrophysiological characterization of drug response in hSC-derived cardiomyocytes using voltage-sensitive optical platforms

Emily R. Pfeiffer-Kaushik, Godfrey L. Smith, Beibei Cai, Graham T. Dempsey, Maria P. Hortigon-Vinagre, Victor Zamora, Shuyun Feng, Randall Ingermanson, Renjun Zhu, Venkatesh Hariharan, Cuong Nguyen, Jennifer Pierson, Gary A. Gintant, Leslie Tung

PII: S1056-8719(19)30027-9
DOI: https://doi.org/10.1016/j.vascn.2019.106612
Article Number: 106612
Reference: JPM 106612

To appear in: *Journal of Pharmacological and Toxicological Methods*

Received date: 23 February 2019
Revised date: 30 June 2019
Accepted date: 10 July 2019

Please cite this article as: E.R. Pfeiffer-Kaushik, G.L. Smith, B. Cai, et al., Electrophysiological characterization of drug response in hSC-derived cardiomyocytes using voltage-sensitive optical platforms, Journal of Pharmacological and Toxicological Methods, https://doi.org/10.1016/j.vascn.2019.106612

Electrophysiological characterization of drug response in hSC-derived cardiomyocytes using voltage-sensitive optical platforms

***Emily R. Pfeiffer-Kaushik[1], *Godfrey L. Smith[2,3], Beibei Cai[1], Graham T. Dempsey[4], Maria P. Hortigon-Vinagre[2,3], Victor Zamora[2,3], Shuyun Feng [1], Randall Ingermanson [1], Renjun Zhu,[7] Venkatesh Hariharan[7], Cuong Nguyen[4], Jennifer Pierson[5], Gary A. Gintant[6], Leslie Tung[7]**

*Both of these authors contributed equally to this work.

Affiliations:

[1]Vala Sciences Inc. 6370 Nancy Ridge Drive, Suite 106, San Diego, CA 92121, USA;

[2]Clyde Biosciences Ltd, BioCity Scotland, Bo'Ness Road, Newhouse, Lanarkshire, Scotland, UK ML1 5UH, United Kingdom;

[3]Institute of Cardiovascular and Medical Sciences, College of Medical, Veterinary and Life Science, University of Glasgow, 126 University Place, Glasgow G12 8TA, United Kingdom;

[4]Q-State Biosciences Inc. 179 Sidney Street, Cambridge, MA 02139, USA;

[5] Health and Environmental Sciences Institute, Washington, D.C., 20009, USA;

[6]AbbVie, 1 North Waukegan Road, Department ZR-13, Building AP-9A, North Chicago, IL 60064-6119, USA;

[7]Department of Biomedical Engineering, The Johns Hopkins University, 720 Rutland Ave., Baltimore, MD 21205, USA.

Corresponding author:

Name: Jennifer B. Pierson

Phone: 1-202-659-3306

E-mail: jpierson@hesiglobal.org

ABSTRACT

Introduction: Voltage-sensitive optical (VSO) sensors offer a minimally invasive method to study the time course of repolarization of the cardiac action potential (AP). This Comprehensive *in vitro* Proarrhythmia Assay (CiPA) cross-platform study investigates protocol design and measurement variability of VSO sensors for preclinical cardiac electrophysiology assays.

Methods: Three commercial and one academic laboratory completed a limited study of the effects of 8 blinded compounds on the electrophysiology of 2 commercial lines of human induced pluripotent stem-cell derived cardiomyocytes (hSC-CMs). Acquisition technologies included CMOS camera and photometry; fluorescent voltage sensors included di-4-ANEPPS, FluoVolt and genetically encoded QuasAr2. The experimental protocol was standardized with respect to cell lines, plating and maintenance media, blinded compounds, and action potential parameters measured. Serum-free media was used to study the action of drugs, but the exact composition and the protocols for cell preparation and drug additions varied among sites.

Results: Baseline AP waveforms differed across platforms and between cell types. Despite these differences, the relative responses to four selective ion channel blockers (E-4031, nifedipine, mexiletine, and JNJ 303 blocking I_{Kr}, I_{CaL}, I_{Na}, and I_{Ks}, respectively) were similar across all platforms and cell lines although the absolute changes differed. Similarly, four mixed ion channel blockers (flecainide, moxifloxacin, quinidine, and ranolazine) had comparable effects in all platforms. Differences in repolarisation time course and response to drugs could be attributed to cell type and experimental method differences such as composition of the assay media, stimulated versus spontaneous activity, and single versus cumulative compound addition.

Discussion: In conclusion, VSOs represent a powerful and appropriate method to assess the electrophysiological effects of drugs on iPSC-CMs for the evaluation of proarrhythmic risk. Protocol considerations and recommendations are provided toward standardizing conditions to reduce variability of baseline AP waveform characteristics and drug responses.

Keywords

1. methods
2. stem cell-derived cardiomyocyte
3. action potential
4. comprehensive in vitro proarrhythmia assay (CiPA)
5. safety pharmacology
6. ICH S7B
7. torsades de pointes (TdP) arrhythmia
8. hERG
9. cardiac electrophysiology
10. voltage-sensitive optical sensors

1. Introduction

The Cardiac Safety Research Consortium (CSRC), the Health and Environmental Sciences Institute (HESI) and the US Food and Drug Administration (FDA) have proposed a new paradigm to assess the clinical potential for pro-arrhythmia risk. The Comprehensive *in vitro* Proarrhythmia Assay (CiPA) initiative is a multi-discipline approach to assaying propensity to arrhythmias: one component consists of evaluating drug actions on multiple cardiac ion channel currents and using this data to reconstruct *in silico* the drug effect on adult cardiac electrophysiology and subsequently to attribute a proarrhythmic score. A second component is designed to confirm the predicted cellular electrophysiological effects of a drug by assay in an *in vitro* cardiac muscle preparation; the consortium suggests the use of human stem cell (hSC)-derived cardiomyocytes (hSC-CM) (Colatsky, et al., 2016; Fermini, et al., 2016; Pierson, et al., 2013; Sager, Gintant, Turner, Pettit, & Stockbridge, 2014; Trepakova, Koerner, Pettit, Valentin, & Committee, 2009). A third component of CiPA investigates biomarkers from the clinical electrocardiogram (J-Tpeak, Tpeak-Tend intervals) (Vicente, Zusterzeel, Johannesen, Mason, et al., 2018; Vicente, Zusterzeel, Johannesen, Ochoa-Jimenez, et al., 2018).

The CiPA initiative follows decades of effort and investment across the pharmaceutical and biotechnology industries and in centers of academic research to develop data-driven *in vitro* screening practices to reduce the risk of proarrhythmic cardiotoxicity in pharmaceutical chemistry. These efforts aim to hold screening assays to appropriately high standards by founding decision-making criteria on well-validated clinically-referenced large data sets (Kramer, et al., 2013; Park, et al., 2018; Pfeiffer, Vega, McDonough, Price, & Whittaker, 2016; Redfern, et al., 2003; Sirenko, et al., 2013). Early efforts to reduce proarrhythmic risk in drug candidates focused on the relationship between inhibition of the I_{Kr} current transmitted through the Kv11.1 (hERG) potassium channel and prolongation of the QT

interval representing cardiac repolarization in the electrocardiogram (ICH_Expert_Working_Group, 2005; Sanguinetti, Jiang, Curran, & Keating, 1995), which is associated with clinical risk of torsades de pointes (TdP) life-threatening arrhythmia. However, subsequent analyses have revealed shortcomings in the accuracy of both hERG-inhibiting drug concentrations (IC50s) and nonhuman preclinical species to accurately predict clinically safe or proarrhythmic compounds at relevant multiples of clinical exposure (Gintant, 2011; Jost, et al., 2013; Park, et al., 2018; Wallis, 2010). The CiPA paradigm proposes to look beyond the hERG channel and animal study paradigm with a mechanistic emphasis to improve the accuracy of preclinical prediction of clinical proarrhythmic risk.

hSC technology introduces a powerful *in vitro* platform for scientific discovery and preclinical evaluation. hSC-derived cells advantageously enable high throughout assessment, strong reproducibility, translation into clinical studies, and potential applications in personalized and precision medicine for many therapeutic areas. Utilization of hSC-derived cells is in agreement with the 3Rs (Replace, Reduce, Refine the need for animal studies) (Beken, Kasper, & van der Laan, 2016; Tornqvist, et al., 2014). The increasing availability of patient- and diverse donor-derived pools of stem cells opens the door to a clinical-trial-in-a-dish paradigm (Fermini, Coyne, & Coyne, 2018; Sayed, Liu, & Wu, 2016; Shinozawa, et al., 2017) .

hSC-CMs have been shown to display cellular electrophysiological properties that are often similar to human primary cardiomyocytes, including ionic currents, channel gating properties, ventricular-like action potentials, and expected sensitivity to multiple drugs (Bett, et al., 2013; Honda, Kiyokawa, Tabo, & Inoue, 2011; Ma, et al., 2011; Peng, Lacerda, Kirsch, Brown, & Bruening-Wright, 2010). A variety of approaches have been utilized in hSC-CM based assays, including patch clamp, microlectrode arrays, optical indicators of voltage, mechanical movement, cellular impedance, Ca^{2+} transients and others (Ando, et al., 2017;

Asakura, et al., 2015; Blinova, et al., 2017; Gossmann, et al., 2016; Guo, et al., 2011; Guo, et al., 2013; Kitaguchi, et al., 2017; Leyton-Mange, et al., 2014; Lu, et al., 2017; Lu, et al., 2015; Nunes, et al., 2013; Pfeiffer, et al., 2016; Pfeiffer, et al., 2017; Piccini, Rao, Seebohm, & Greber, 2015; Puppala, et al., 2013; Scott, et al., 2014; Sirenko, et al., 2013; Sun & Nunes, 2016; Zeng, Roman, Lis, Lagrutta, & Sannajust, 2016). These studies have provided promising evidence that hSC-CMs are a relevant cell model to study drug-induced cardiac abnormalities, including arrhythmia and QT prolongation, and display good *in vitro* concordance to clinical findings.

Among the diversity of detection methods, a number of optical assays have been developed to visualize cardiomyocyte electrophysiology with voltage (transmembrane potential; cardiomyocyte action potential (AP))-sensitive fluorescent dyes and to perform real time recordings of hSC-CMs (Blazeski, et al., 2018; Lu, et al., 2017; Lu, et al., 2015; Passini, et al., 2017; Pfeiffer, et al., 2016; Pfeiffer, et al., 2017; Shadrin, et al., 2017; Sirenko, et al., 2013; Zeng, et al., 2016). In addition to chemical dyes, fluorescent proteins have been bioengineered to either report fluorescence in response to cellular electrophysiology (genetically encoded voltage indicator; GEVI, or genetically encoded calcium indicator; GECI), or to alter cellular electrophysiology in response to illumination (optogenetic stimulation) (Klimas, et al., 2016; Shinnawi, et al., 2015; Xu, Zou, & Cohen, 2017). Compared with more traditional methods like patch clamp and field potential recording, these optical platforms often have the advantage of higher throughput (e.g., versus patch clamp) and the possibility of simultaneous detection of multiple aspects of cardiomyocyte electrophysiology, including beat rate, action potential duration (APD), triangulation of repolarization, conduction velocity, etc.

As methods for assaying cardiac electrophysiology in hSC-CMs become more commonplace and the scale of use expands from individual laboratories to a broader

pharmaceutical and regulatory context, it is important to understand the degree to which the diversity in methods across platforms, protocols, and laboratories may create inconsistencies in results. In order to compare results gained from different methods, especially for predictive values, it is critical to have either a standardized protocol in place, or a framework for data contextualization per method and across time. Factors which may influence results of cell-based *in vitro* assays such as those using hSC-CMs include but are not limited to: cell line and production lot variance, adhesion matrix coating protocol (if applicable), cell plating density, culture duration, culture medium, dye selection, assay conditions, and data interpretation. (These factors would also contribute to discrepancies in any assay involving cell lines recombinantly expressing hERG or any other ion channel or receptor of interest).

This is a report of a CiPA hSC-CM action potential cross-platform study initiated by the CSRC, HESI and FDA to evaluate experimental protocols and assess the variability and discriminating power of fluorescence-based electrophysiological signals obtained from commercial hSC-CMs. The goal of the study was to provide exemplar proarrhythmia assay data with a diverse selection of optical methods for recording the cardiomyocyte action potential, utilizing the same, well characterized, reference compounds at the same concentrations, tested in hSC-CMs of identical production lots, as a first step toward cross-site standardization of protocols or validation frameworks. Each site measured and reported the same action potential parameters (e.g. beat rate and specified action potential durations). The study measured the effects on the action potential (AP) of hSC-CMs using a limited number (8) of well-known drugs and limited replicates (n=3 replicate wells or 1 large size monolayer per condition) and four different optical systems designed for medium throughput. The study was administered by the CiPA Myocyte Subgroup and involved three commercial enterprises (Clyde Biosciences Ltd UK, Vala Sciences Inc USA, and Q-State Biosciences Inc USA) and one academic laboratory (Cardiac Bioelectric Systems Laboratory, Johns Hopkins

University, USA) using a variety of optical methods and voltage sensors. The results show that features of depolarization and repolarization including action potential shape could be resolved by all platforms involved in the study, and that experimental conditions and the form of optical measurement system are critical variables in defining a standardized cellular response.

2. Material and Methods

2.1. Cell plating and culture conditions

As determined by the CiPA Working Group, the core sites involved in the study were provided with frozen cell material from matched batches of 2 commercial cell lines. All groups received cells from two manufacturers namely Cor.4U® cardiomyocytes (lot CB142CL_V_4M) (Ncardia, formerly Axiogenesis), Cologne, Germany) and iCell™ cardiomyocytes (catalogue number CMC-100-010-001; donor 01434; lot 1093711) (Cellular Dynamics International, WI, USA). The culture conditions used by each group for Cor.4U and iCell cells are given below.

Clyde Biosciences: Cor.4U and iCell cardiomyocytes were kept in liquid nitrogen until culture according to the instructions provided by the respective manufacturers. In both cases, the cells were cultured in 96-well glass-bottomed plates (MatTek, Ashland, MA, USA; Cat. No. P96G-1.5-5-F) coated with fibronectin (70µl/well at 10µg/ml in PBS [+Ca^{2+} & Mg^{2+}]) (Sigma-Aldrich, St. Louis, MO, USA; Cat. No. F-1141) in an incubator at 37°C for 3h. The cell density for Cor.4U and iCell cardiomycytes were $0.78\times10^5/cm^2$ (25,000 cells/well after adjustment by the manufacturer's lot plating efficiency), the subsequent maintenance protocols followed manufacturer's instructions and the corresponding maintenance media (Cor.4U: Cor.4U®-maintenance media; iCell: iCell™-maintenance media). Experiments were

performed between days 4-8 (Cor.4U) and 10-15 days (iCell) post-thaw as recommended by the manufacturers, using media reported in **Table 1** and **Supplemental Table 1**.

Johns Hopkins University: Cor.4U and iCell cardiomyocytes were seeded onto 35mm plastic tissue culture dishes (#353001, BD Biosciences) as confluent monolayers for optical mapping. To match the size of the monolayer to the optical mapping field of view, the growth area of the 35mm dishes was restricted to a 10mm diameter circle by filling the 35mm dishes with a polydimethylsiloxane (PDMS) stencil, in which a 10mm diameter circular hole was punched out at the center, exposing the tissue culture-treated surface for monolayer culture. The 35mm dishes were then UV-sterilized and coated with Geltrex (#A1413302, Thermofisher, at 1:100 dilution) overnight before use. Cor.4U and iCells were prepared according to the manufacturers' specifications. For Cor.4U cardiomyocytes, cells were thawed in manufacturer-provided medium according to manufacturer instructions and maintained for two days to allow recovery from cryopreservation. These cells were then dissociated, counted and plated at $1.60\times10^5/cm^2$ (127,000 cells/well) to form confluent monolayers (which were not formed at the lower manufacturer's recommended density). The monolayers were cultured in manufacturer-provided medium for an additional 8 days prior to optical mapping. For iCell cardiomyocytes, cells were thawed, counted and plated at $2.55\times10^5/cm^2$ (200,000 cells/well) to form confluent monolayers. The monolayers were cultured in manufacturer-provided medium for 10 days prior to optical mapping. Two μg/ml ciprofloxacin was added to the media throughout culture of the Cor.4U cardiomyocytes, and 25 μg/ml gentamycin was added throughout culture of the iCell cardiomyocytes per manufacturer recommendations.

Q-State Biosciences: Cor.4U and iCell cardiomyocytes were cultured in six-well plates (VWR, Radnor, PA, USA; Cat. No. 353046) coated with 0.1% gelatin (Millipore, Taunton,

MA, USA; Cat. No. ES-006-B) following manufacturer's instructions. The cells were transduced to express the components of the optogenetic-GEVI construct Optopatch, which consists of CheRiff, a blue-light activated channelrhodopsin actuator, and QuasAr, a red light voltage reporter (Hochbaum, et al., 2014). Three (for Cor.4U) to five (for iCell) days after plating, hSC-derived CMs in each well were transduced overnight with custom made lentivirus for expression of CaViar (fusion construct of GEVI QuasAr2 and GECI GCaMP6f) or CheRiff (optogenetic channel). Virus was removed from the cells and maintenance medium added to each well. At 6 days post-thaw, to enable the option of simultaneous voltage and Ca^{2+} imaging with optical pacing using Optopatch, the CheRiff-expressing cells and CaViar-expressing cells were dissociated and re-plated into the same dish. CheRiff-expressing cells were replated in the periphery and CaViar cells were replated in the center of each dish, as described previously (Dempsey, et al., 2016). Briefly, one side of a PDMS disc was treated with 10µg/mL fibronectin (Sigma-Aldrich, St. Louis, MO, USA; Cat. No. F2006) in 0.1% gelatin for 10 min at room temperature, dried and then pressed offset to one side onto a MatTek dish (Ashland, MA, USA; Cat. No. P35G-1.5-10-C). The remaining area was coated with 10µg/mL fibronectin in 0.1% gelatin overnight. CheRiff-expressing cells were trypsinized according to the manufacturer's instructions and ~10,000 cells added to the exposed glass surface for 40 minutes at 37 °C in 5% CO_2. Discs were removed, and the dish was washed with 150µL of maintenance medium. CaViar-expressing cells were trypsinized according to manufacturer's instructions then re-plated overnight to a final density of 0.7×10^5 cells/cm^2 (45,000 additional cells/well). Maintenance medium (1.0 mL) was added to each dish, and media changes were conducted according to the manufacturer's instructions. Cells were imaged 7-10 days (Cor.4U) and 14-17 days (iCell) post-thaw as recommended by the manufacturers.

Vala Sciences: Cor.4U and iCell cardiomyocytes were thawed and cultured in accordance with protocols suggested by the cell manufacturer, in 96 well plates featuring optically clear well bottoms (Cat. No., 655090, Greiner, Monroe, NC, USA). Cor.4U cardiomyocytes were plated at 1.40×10^5/cm^2 (45,000 cells/well) on culture surfaces coated with fibronectin (10µg/mL, Cat. No. F1141, Sigma-Aldrich, St. Louis, MO, USA), in plating media including 0.5 mg/mL puromycin, both provided by the cell manufacturer, and maintained at 37°C and 5% CO_2. The media was changed to the manufacturer's maintenance media three hours after plating, replaced after 24 hours and every subsequent two days until assay of the Cor.4U cardiomyocytes after six days of culture. iCell cardiomyocytes were plated at 0.78×10^5/cm^2 (25,000 cells/well), calculated after applying the manufacturer's plating efficiency (0.55) for the lot, on surfaces coated with 250µg/ml Matrigel (Corning 356237, Fisher Scientific, Waltham, MA, USA). The cells were maintained for the first two days in plating medium provided by the manufacturer at 37°C and 7% CO_2. The media was replaced with maintenance media provided by the manufacturer supplemented with 25µg/ml gentamicin (Gibco, Waltham, Massachusetts, USA) every two days, and with antibiotic-free media 24h before assay. iCell cardiomyocytes were maintained in culture for 10 days prior to Kinetic Imaging Cytometry (KIC) assay. Both lines of cardiomyocytes displayed spontaneous beating within 48h of thawing and maintained this phenotype throughout the duration of the experiment.

2.2. Optical recordings and compound testing

Clyde Biosciences: On the day of experiments cells were washed in serum free media the composition of which differed for the two cell types: Cor.4U cardiomyocytes were exposed to BMCC media (Bohlen Modified Complete Culture, NCardia Ax-M-BMCC250); iCell cardiomyocytes to DMEM (Dulbecco's Modified Eagle Medium, Gibco 11966) supplemented with 10mM galactose and 10mM sodium pyruvate as per manufacturers'

instructions (**Supplemental Table 1**). hSC-CMs were loaded with 6μM di-4-ANEPPS (Biotium; Cat. No. 61010) in serum-free media (SF media) for one minute at room temp. Cells were then washed in indicator-free cell specific SF media and stored in an incubator for 2h prior before experimentation. The multi-well plate was placed on a stage incubator (37°C, 5% CO_2, water-saturated air atmosphere OkoLabs Inc, USA) of the CellOPTIQ platform (Clyde Biosciences Ltd, Glasgow, Scotland). The di-4-ANEPPS signal was recorded by a PMT from an area 0.2 x 0.2 mm using a 40x (NA 0.6) objective lens. Baseline spontaneous activity was recorded by capturing a 15-20s segment of fluorescent signal and this was repeated 30min after exposure to the drug or vehicle (DMSO). Drugs were tested at four concentrations (N=3 for each concentration) with matched vehicle controls (0.1% DMSO) for each concentration, added at 5X concentration by removing 20% volume and replacing with drug. Fluorescence signals were digitized at 10 kHz. Offline analysis was performed using proprietary software (CellOPTIQ).

Johns Hopkins University: On the day of drug testing, cultures were transferred to Tyrode's solution (**Supplemental Table 1**). Monolayers were stained in Tyrode's solution containing 10μM voltage sensitive dye di-4-ANEPPS (D1199, Invitrogen, Grand Island, NY) for 10min. The PDMS cell culture stencil was removed from the 35mm culture dish after brief rinse of the monolayer, and then 2mL of Tyrode's solution was added to the culture dish prior to test compound treatment and optical mapping. For Cor.4U monolayers, 10μM of blebbistatin (B0560, Sigma-Aldrich, St. Louis, MO) was also applied to inhibit motion. Experiment temperature was controlled at 37°C by using a heated stage throughout the recordings. Electrical stimulation was applied through a pair of platinum electrodes placed at the edge of the monolayer. Optical action potentials were recorded using a MiCAM Ultima-L CMOS camera (SciMedia, Costa Mesa, CA) with tandem 1x Plan Apo lens (Leica, with 0.44

NA). The field of view was 1 x 1 cm and had 100 x 100 pixel spatial resolution at 500 frames/sec. Each pixel represented an area of approximately 0.1mm x 0.1mm.

Stock solutions of all compounds were prepared in DMSO (vehicle) according to protocols provided for CiPA studies, which is at 1000x the highest testing concentration. The stock solution was diluted in Tyrode's solution at 1:100 for optical mapping. For DMSO control, 1:100 DMSO was prepared in Tyrode's solution. The final concentration of DMSO was <0.1% at all times. Untreated baseline, then 4 test compound concentrations were recorded for each test article (test compound, or vehicle control) sequentially. Ten minutes were allowed between each compound concentration for the compound to reach steady-state effects before recording optical action potentials. Optical action potentials were analyzed using custom MATLAB programs. The region of monolayer analysed was automatically determined based on signal-to-noise ratio of action potentials recorded from individual sites, and approximately 7000 measurements were made per monolayer. A sliding 5 × 5 pixel Gaussian filter was applied spatially to improve signal quality across the field of view. Because of the large number of cells required per monolayer and extensive manual aspects of the experimentation, technical replicates were performed only at baseline; otherwise it was one monolayer per test condition. Action potential parameters as described in Data Analysis were calculated using MATLAB routines.

Q-State Biosciences: Prior to imaging, medium was removed from the dish and 1.5 mL of warmed maintenance medium without phenol red, vitamins and amino acids was added (**Supplemental Table 1**). Cells were kept at 37°C in 5% CO_2 for 30 minutes prior to imaging. Imaging was performed on a microscope custom-built to actuate and record Optopatch. Cells were maintained at 37 °C with a heated stage (Warner Instruments) and objective collar (Bioptechs), and 100% humidity at 5% CO_2. The imaging protocol comprised the following: spontaneous activity (30s), followed by activity at 1 Hz and 2 Hz pacing (15s

each), repeated in two different fields of view within each dish. Drug addition within each dish included a vehicle (DMSO) control, followed by cumulative ascending concentration (four test concentrations, three replicate dishes per concentration, 10 minute treatment time per concentration) by removing 10% of the dish volume and adding the drug at 10X the final concentration. Pulses of blue LED illumination (6 ms, 0.5 W/cm^2, λ = 488 nm) were used to pace the CMs by stimulating CheRiff in the peripheral cells. Blue laser light (λ = 488 nm, 0.15 W/cm^2) and red laser light (λ = 640 nm, 50 W/cm^2) excited fluorescence of GCaMP6f and QuasAr2, respectively, in the central cells (QuasAr2 providing transmembrane voltage data, the subject of this study). Fluorescence was collected with a 20x water immersion objective (NA1.0). An illumination area of ~200 μm x 200 μm was used to image cardiomyocytes and generate the traces used to compute action potential statistics. A dual-view system projected emission from GCaMP6f and QuasAr2 onto adjacent halves of a sCMOS camera (Orca Flash 4.0, Hamamatsu), operating at a frame rate of 500 Hz. The signals from the 500x500 pixels of the camera were averaged together to obtain the AP and its parameters, and 3 areas were measured and averaged per well. Voltage and calcium traces were scaled to fractional changes in fluorescence relative to baseline ($\Delta F/F$). In the current study, only voltage data from spontaneously active and 1Hz stimulation was used to compare with the 3 other platforms.

Vala Sciences: Cardiomyocytes were loaded with FluoVolt and PowerLoad (Invitrogen, Cat. No. F10488, Carlsbad, CA, USA) per manufacturer instructions, in a loading buffer of 20mM HEPES in HBSS and 200ng/mL Hoechst 33342. Cells were loaded for 30 minutes at 37°C. Stock solutions of each blinded compound test concentration were prepared in DMSO at 1000-fold the test concentration, aliquoted and stored at -80°C. High content analysis was conducted using an IC-200 Kinetic Image Cytometer (KIC; Vala Sciences, San Diego, CA). Compounds were diluted to final concentration in Tyrode's solution (**Supplemental Table**

1). Following dye loading, the cells were washed with 37°C Tyrode's solution. The compounds or vehicle (DMSO) control, diluted to their final test concentrations in 37°C Tyrode's solution, were then 100% exchanged with solutions in the appropriate wells. Compound treatments were performed in triplicate wells and compared against 6 replicate in-plate vehicle control wells. For the experiment with Cor.4U cardiomyocytes, a total of 33 replicates of vehicle control were used, and for the experiment with iCell cardiomyocytes, a total of 36 replicates of vehicle control were used. A final DMSO concentration of <0.1% was maintained in each well assessed in the study. The cardiomyocytes were incubated with test compounds at 37°C for 20 minutes prior to being imaged. A KIC was used to capture movies of the action potentials, described previously (Cerignoli, et al., 2012; Lu, et al., 2015). The environmental control chamber of the KIC was set to 37°C. For these experiments the KIC was fitted with a 20x NA 0.75 objective and captured one image of the nuclei (Hoechst), then recorded 20 sec of action potential activity (FluoVolt) at 30 frames/sec from each well. An area of 0.58 x 0.58 mm^2 of cells was recorded for each well. Action potential analysis was performed using CyteSeer automated image analysis software (Vala Sciences Inc., San Diego, CA, USA). Briefly, the FluoVolt intensity of around 1785 x 1785 pixels within a field of view of 0.58 x 0.58 mm2 was averaged to obtain an AP trace that was used to determine the reported per well values.

A summary of the optical platforms, and the VSO sensor, type of pacing, plating density, media, detector and acquisition rate for all four test sites is given in **Table 1**. The drugs used and their concentration and ion channel targets are shown in **Table 2**.

2.3. Drug list and stock preparation

The CiPA Myocyte Subgroup selected eight compounds for the cross-platform study (**Table 2**). Compounds were distributed blinded by National Cancer Institute (U.S. Department of Health and Human Services) to all participating sites with instructions for

preparation in DMSO (also provided from a common stock) and instructions on the four dilutions to be used in the study. The compound set included four ion channel-selective compounds to test inhibition of I_{Na} (mexiletine), I_{CaL} (nifedipine), I_{Kr} (E-4031), and I_{Ks} (JNJ 303), and four mixed ion current blocking agents flecainide, moxifloxacin, quinidine, and ranolazine. Although mexiletine has hERG inhibitory properties (Supplemental Table 4), it was not classified as inducing TdP risk by the CiPA Myocyte Subgroup on the basis of its categorization in the QTDrugs Lists at CredibleMeds® (known risk of TdP or other categories, https://crediblemeds.org) (Supplemental Table 3).

2.4. Data Analysis

The average AP waveform was generated based on a minimum of 15 sec continuous record of spontaneous and/or stimulated APs. The following parameters were measured: action potential rise time (Trise) i.e. time from 10% to 90% of the upstroke; action potential duration (APD) at 3 points on the repolarisation phase (30%: APD_{30}, 60%: APD_{60} and 90%: APD_{90}); a triangulation index (APD_{90}-APD_{30}; Triang) or normalized triangulation index (Triang/APD_{90}); and average cycle length (CL) or beat rate (BR) were also recorded.

Unusual AP configurations which suggested altered excitability or predisposition to arrhythmia-like events were observed on addition of some drugs. These events were recorded according to a category of event based on waveform shape as shown in **Supplemental Figure 1**. This shows different examples of arrhythmia-like AP waveforms and quiescence.

2.5. Statistics

Statistical analysis was performed using ANOVA followed by Dunnett's test following ANOVA to allow the comparison of a number of treatments with a single control. Statistical significance was designated as * $P<0.05$, ** $P<0.01$, *** $P<0.001$, **** $P<0.0001$.

3. Results

3.1. Baseline values

Examples of optical recordings measured at each of the four test sites are shown in **Figure 1** for Cor.4U and iCell cardiomyocytes. The average (mean), standard deviation (SD), and coefficient of variation (CoV) for the AP waveform parameters for both cell types recorded on the 4 platforms without test compound treatment is given in **Table 3**. At three sites (Clyde, Q-State and Vala), spontaneously beating cells were recorded. One of the sites (Q-State) also recorded with electrical stimulation to control beat rate (1 Hz), and at the fourth site (JHU), only stimulated (1 Hz) recordings were made. CoV of cycle length values recorded from spontaneously active cells (0.11-0.65) may be used as a measure of the regularity of the spontaneous beating. APD_{90} CoV was less than 0.25 for all methods and cell types. There were marked differences in both depolarization and repolarization characteristics across sites and cell types. The smallest differences appeared within cell type and between sites using comparable media composition, e.g. Q-State and Clyde used similar media compositions for iCell recordings and the range of CL and APD values was comparable in both groups. The Tyrode's solution used at the Vala and JHU sites had similar composition. At the Vala site, which did not utilize beat rate control, cycle length and APD_{90} for iCell tended to be longer and less variable than at the other sites (Clyde and Q-State) with spontaneous recording, whereas at the JHU site, which controlled beat rate with 1 Hz stimulation, iCell APD_{90} was more similar to the sites with shorter cycle length (Clyde and Q-State). For Cor.4U, spontaneously beating cells at the Q-State site tended to have longer cycle lengths than at the Clyde and Vala sites. Shorter cycle lengths coincided with fewer post-thaw days of culture for Cor.4U (range 4-10 days), but not for iCell (range 10-17 days). A limitation of beat rate control is that it can be performed only at rates greater than the

spontaneous beat rate (overdrive pacing), which may be altered by drug-induced electrophysiological changes.

Figure 2 shows the relationship between the cycle length obtained from spontaneously active and 1Hz stimulated cells and the associated APD_{90}. Panel A shows the data from all 4 sites for Cor.4U cardiomyocytes, and panel B the data for iCell cardiomyocytes. The cycle length vs. APD_{90} relationship for the combined dataset from all four sites was roughly co-linear for iCell cardiomyocytes, which suggests an underlying linear relationship unaffected by variations in experimental conditions at the four sites. In contrast, the overall Cor.4U cycle length vs. APD_{90} relationship was not linear, across or within sites. Cor.4U cells were recorded in the same media as iCell recordings at all except the Clyde site. **Table 4** lists the regression equation for the combined dataset, and the regressions for the spontaneously beating datasets of individual sites are listed in **Supplemental Table 2**. For iCell cells, the slope for all 3 groups was approximately 0.1. The slope for Cor.4U cells for both Clyde and Vala was approximately 0.1, but Q-State data did not fit this relationship.

Rise time values ranged widely and appeared broadly inversely correlated with acquisition rate (**Table 3)**, with TRise ranging from approx. 6ms (iCell Clyde site) to approx. 40ms (iCell Vala site). The response time constant of a VSO can potentially limit the temporal resolution of data collected in optical assays. However, the VSOs utilized in this study have relatively fast kinetics (**Table 1**) which should not be limiting to the features measured in this study: (< 1 ms) di-4-ANEPPS (Loew, et al., 1992), (< 1 ms) FluoVolt (VoltageFluor2.1) (Miller, et al., 2012), (< 3 ms) QuasAr2 (Hochbaum, et al., 2014). Rise time may also be proportional to the size of the area of sampled cells, because of the time delay for the depolarization wave to propagate across the measurement area, but this was not found to be the case. Q-State, which had the smallest sampling area of 0.4μm x 0.4μm (**Table**

1), had longer Trise than Clyde, which had a much larger sampling area of 0.2mm x 0.2mm but the shortest rise times and highest acquisition rate. On the other hand, within cell type, spontaneously beating hSC-CM TRise bore a positive relationship to cycle length that was linear for iCell cells, and a broad positive correlation to the concentration of NaCl (range 86 mM – 135 mM) and total sodium ion (range 110 mM – 175 mM) in the extracellular imaging solution (**Supplemental Table 1**).

3.2. The effect of vehicle on electrophysiological parameters

Figure 3A shows an example of the effect of DMSO vehicle on the voltage signals from hSC-CMs. An example of the average effects of the vehicle on a range of parameters (cycle length, APD_{90}, triangulation and rise time) from a single site (Clyde) is shown in **Figure 3B**. CL and APD_{90} showed no effect with minimal variation, while triangulation and TRise were more variable. The mean values showed no difference from zero, and this was consistent for both cell types used in the study. As shown in **Figure 3C** for the values of APD_{90}, DMSO had similarly minimal effects on average AP characteristics across all the sites. One site (Vala) did not make baseline measurements in the absence of vehicle.

3.3. Example of the electrophysiological response to 4 selective ion channel blockers

An example of the change in AP parameters caused by the four selective ion channel drugs (E-4031, nifedipine, mexiletine, and JNJ 303) is shown for one site (Clyde) in **Figure 4**. Panel A shows example traces before and 30 minutes after addition of a single concentration of the drug. E-4031 prolonged the action potential in both cell types with marked increases in triangulation indicating prolongation of the late repolarisation phase. Nifedipine shortened both cycle length and APD_{90} while mexiletine caused significant changes in APD and tended to increase cycle length. Trise was also altered by compound treatment, albeit in a more variable and frequently bidirectional manner. The I_{Ks} blocker JNJ

303 showed no significant effects in Cor.4U cardiomyocytes but reduced cycle length in iCell cardiomyocytes with few other significant effects on the waveform shape.

3.4. Summary of effects of all 8 CiPA compounds on the AP waveform across all sites

All eight (blinded) compounds (**Table 2**) were applied at each site to iCell and Cor.4U cells. These were applied at two sites (Clyde and Vala) at a single concentration per well, and at the other two sites (JHU and Q-State) using cumulative concentrations in the same wells. For brevity and illustration, **Figure 5** compares the results for the 8 tested compounds (**Table 2**) across all sites for the key repolarization parameter (APD_{90}). The results for all other measured parameters (spontaneous cycle length, APD_{30}, APD_{60}, rise time, triangulation, normalized triangulation) can be found in **Supplemental Figure 2**. Depending on the test site, action potential recordings were obtained during spontaneous activity and/or electrical or optical pacing. Generally, the potent hERG inhibitors E-4031, flecainide, and quinidine (**Supplemental Tables 3 & 4**) prolonged the action potential recorded from both Cor.4U and iCell cardiomyocytes in a concentration-dependent manner, and/or caused arrhythmias or stopped beating, consistent with the blockade of repolarizing I_{Kr}. Nifedipine caused a concentration-dependent reduction in APD_{90}, consistent with inhibition of I_{CaL}. JNJ 303 caused little to no alteration in APD_{90}. For compounds with mixed ion channel inhibition, some differences in sensitivity to sodium and calcium channel inhibition are apparent, with some preparations (per cell type and experimental protocol) more reflective of a hERG inhibitory effect, and others more sensitive to an inward current inhibition (e.g. quinidine 3-10 μM). Differences in experimental protocol (e.g. cell density or compound exposure duration) may influence these differences in sensitivity. However, despite the differences in cell type, media composition and spontaneous/stimulated beat rate as well as cumulative vs. individual dosing protocols, there was broadly consistent drug effect across sites.

3.5. Incidence of arrhythmia-like events

Arrhythmia-like events were documented per the agreed key (**Supplemental Figure 1**). The reported incidence and class of events are shown in **Table 5**. The low number of drugs, sites, and cell lines tested in this cross-platform study makes statistical comparisons of limited value, but consistent trends were clear. A comparison of the channel inhibition IC50s of each compound, as well as their clinical exposure are listed in **Supplemental Tables 3 & 4**. The compound concentration ranges that induced arrhythmia-like events in this study are also listed. Generally there was some consistency across sites: all sites reported events using the hERG blocking drugs E-4031 and quinidine, which are known to cause QT prolongation and high TdP risk. No site observed arrhythmia-like events with JNJ 303 and moxifloxacin. Nifedipine caused quiescence or a tachyarrhythmia (high frequency activity typically lacking normal action potential morphology) at 3 out of 4 sites in the concentration range that was about 2-fold above the IC50 of Cav1.2, and at least 3-fold higher than the therapeutic exposure. Because Cav1.2 is strongly inhibited at these concentrations, APD decreases, permitting rapid reactivation due to high frequency focal activity or re-entrant activity. Ranolazine cause arrhythmia-like events at only one site, at concentrations relevant to hERG inhibition and at the top of the QTc-prolonging clinical exposure range. Flecainide and mexiletine were associated with arrhythmia-like events in 3 out of 4 sites, flecainide at near the clinically QTc-prolonging concentration, and mexiletine at 10- to 20-fold above the therapeutic exposure. Overall, the test concentrations at which the drugs caused arrhythmia-like events were comparable with the ion channel IC50s (within 3-fold), and for the 7 drugs tested clinically, test concentrations producing arrhythmia-like events were in agreement with QTc measurements and documented arrhythmia at that exposure. These observations demonstrated that with protocol optimization, VSO platforms can be a useful tool for assessing drug-induced arrhythmia in clinically relevant concentration ranges.

4. Discussion

The goal of this cross-platform study was to assess the variability among four different sites using various VSO techniques to measure action potential changes in response to a panel of eight drugs with well-known electrophysiological effects. Efforts were made to standardize the test conditions by using identical batches of the same commercial cell lines, manufacturer-provided plating and maintenance media, and drug stocks prepared and deidentified by a third party. At all sites, drugs were tested in serum-free media to avoid uncertainty due to drug binding to protein in the media. Because of the small number of sites, statistical tests of differences were not feasible. Nevertheless, with a few exceptions, the drug responses were quite similar (**Figure 5**), despite differences in voltage sensors, optical measurement systems, and experimental conditions (plating density, imaging solution, pacing conditions, method of compound addition) as summarized in **Table 1**. Furthermore, despite noted differences in some electrophysiologic characteristics of hSC-CMs vs. acutely isolated native human ventricular myocytes, these studies demonstrate the ability to detect delayed and altered cellular repolarization, as has been demonstrated previously (Casini, Verkerk, & Remme, 2017; Jonsson, et al., 2012).

Some observations can be gleaned from the experimental data of the four sites. In general, APDs were longer for iCell than for Cor.4U cardiomyocytes (**Figure 1**, **Table 3**). For cells that were spontaneously beating, APD_{30} and APD_{90} were longer for Vala (iCell only), and for cells that were paced they were longer for JHU (**Table 3**). These two sites assayed drug effects in Tyrode's solutions, which are commonplace in electrophysiological research, while the other two sites used serum-free medias (**Table 1, Supplemental Table 1**) with unique ionic and biochemical composition which may influence baseline cardiomyocyte electrophysiological characteristics. When plotted against the cycle length of the spontaneous

beat rate, the differing APD_{90} exhibited a common linear relationship (**Figure 2**) for iCell cardiomyocytes (approx. 0.1 ms APD_{90} per ms cycle length), but not for Cor.4U cardiomyocytes, although for two out of three of the spontaneously beating sites, the intra-site regression also had a slope of ~ 0.1.

The effects of the eight test compounds on APD_{90} were similar in both cell lines, in at least three and sometimes in all four of the test sites (**Figure 5**). Effect sizes tended to be suppressed when beat rate was controlled (1Hz), versus in spontaneously beating cardiomyocytes. With increasing doses, little or no change in APD_{90} was observed with JNJ 303. APD_{90} decreased with nifedipine (~ 30-50%). For compounds which have been observed to inhibit hERG (**Supplemental Table 4**), APD_{90} increased with a range of effect size relevant to TdP risk classification: smaller effects with mexiletine (typically < 50%; at highest test concentration, >50% in iCell at 2 sites and Cor.4U at 1 site, or stopped beating in iCell at 2 sites), ranolazine (~ 50-150%), and moxifloxacin (Cor.4U tended >50%), compared with a larger effect for E-4031, quinidine, and flecainide (in spontaneously beating cells, typically >100% and/or instances of stopped beating and arrhythmia). In compounds which inhibit multiple ion channels, for example quinidine, which has potency against hERG relevant to the lower concentrations tested here and potency against Nav1.5 and Cav1.2 near or above the higher concentrations tested here, relative sensitivity to inhibition of repolarizing or depolarizing currents may be influenced by experimental protocol. Overall, despite the systematically longer action potentials observed in iCell compared with Cor.4U cells, the changes in action potential parameters of both cell lines to test compounds were generally similar with regard to percent change (**Figure 5** and **Supplemental Figure 2**).

The incidence of these arrhythmia-like events as defined in **Supplemental Figure 1** (**Table 5**) was lowest for JHU, as the only site which used 1 Hz pacing and large (cm) sized cell monolayers, and lower at Q-State in paced versus spontaneously beating iCell. E-4031

and quinidine elicited events across all four sites in at least one cell line. Excluding JHU, these events also tended to be more frequent across sites for iCell compared with Cor.4U cardiomyocytes. The tendency of compound addition to stop cardiomyocyte spontaneous beating was increased in relation to the concentration at which compounds in an intermediate stock solution were added to the cells (i.e. 5X, 10X), versus full media exchange at compound dosing (1X). Cumulative dosing, and post-thaw handling (trypsinization & re-plating, viral infection for transgene expression) may additionally contribute to this effect.

Action potential measurements are traditionally obtained from cardiac tissues or individual cells using glass microelectrodes (e.g. whole cell clamp using glass micropipettes). However, this approach is extremely labor-intensive and is very low throughput, while the demands of a screening assay require at least medium throughput to efficiently assay drugs at the scale of commercial drug discovery and risk evaluation. To improve the throughput, automated patch clamp can be employed as a proven high throughput assay (Rajamohan, et al., 2016; Scheel, et al., 2014). However, measurements of action potentials and APD are highly sensitive to the quality of the seals that can be obtained with the cells, and artifacts can also be introduced via dialysis of solutions into the cell.

At present, the primary methods for evaluating drug effects on the action potential of hSC-CMs are with field potential and fluorescent action potential recordings. Many investigators and organizations use extracellular multielectrode arrays (MEAs) to measure both the hSC-CM beat rate and the field potential duration. Under ideal recording conditions, the field potential is described as a second order filtered version of the action potential (Tertoolen, Braam, van Meer, Passier, & Mummery, 2018). In this description, field potential spike corresponds to the action potential upstroke, and field potential duration (measured as time from positive peak of spike to positive peak of repolarization wave) is theoretically linearly related to APD_{90} (Tertoolen, et al., 2018). However, it is the time course of

repolarisation of the action potential that is indicative of the pro-arrhythmic potential of a compound (Hondeghem, 2008; Hondeghem, Carlsson, & Duker, 2001). Action potential measurements provide more detailed information than is available from field potential reordings, such as AP rise time (a measure of fast sodium channel activity), AP duration at different levels of repolarization (APD_{30}, APD_{60}, APD_{90}) and triangulation (duration of late repolarization (Hondeghem, et al., 2001), measured in this study as the difference between APD_{90} and APD_{30}). As a measure of late repolarization, triangulation has previously been used as one of several metrics comprising a quantitative index of arrhythmia risk in the TRIaD assay, an *ex vivo* whole heart action potential study (Hondeghem, 2008). Transmembrane voltage signals obtained using VSO sensors can measure the effects of a drug on the complete action potential waveform (Blazeski, et al., 2012; Dempsey, et al., 2016; Klimas, et al., 2016), although absolute values of transmembrane voltage are generally not accessible. While the use of VSO dyes can limit the duration of recording time possible, the relatively homogeneous and sensitive nature of the commercially available hSC-CMs studied here afford measurement of electrophysiological effects with high temporal and membrane potential differential resolution from relatively short duration recordings (< 20 sec), supporting discrimination among APD_{30}, APD_{60}, APD_{90}, whereas this resolution is lost in measurement of field potential by MEA. Instability of the action potential plateau phase (oscillatory EADs) are clearly resolved using VSO methods, but can be more difficult to detect in MEA field potential recordings. The signal quality in MEA, and apparent field potential amplitude, is highly dependent on the strength of contact between the cell and measurement electrode, which can vary from electrode to electrode within the same well, and as a result of compound effect. Optical measurement platforms can be used to routinely perform medium throughput measurements of the electrical activity of hSC-CMs as intended

by the CiPA initiative, and can support test article versus vehicle assessments at more chronic exposures.

In a companion CiPA cross-platform study using MEA technology conducted in parallel to this one, recordings 2-5 minutes in duration were collected in spontaneously beating cells before and after a 25 minute test compound treatment, and criteria for inclusion were set to eliminate datasets which did not detect ≥20% increase in rate-corrected field potential duration FPDcF in response to I_{Kr} inhibitor E-4031 or ≥20% decrease in FPDcF in response to I_{CaL} inhibitor nifedipine (Millard, et al., 2018). Eight of 18 participating sites were excluded from the final analysis for having failed to meet this inclusion criteria. While the same compounds and test concentrations were used in the CiPA VSO and MEA cross-platform studies, a direct comparison is limited due to differences in protocol (MEA platforms used serum-containing media, while VSO platforms used serum-free media) and analysis (the MEA study chose to present FPD data as FPDcF, corrected by the empirically-derived Fridericia formula for correcting the QT interval of the clinical electrocardiogram on the basis of heart rate). However, it should be noted that in this study the VSO datasets were overall successful in detecting I_{Kr} and I_{CaL} inhibitor effects. All data sets in this study detected > 20% increase in APD_{90} in response to E-4031, and all spontaneously beating data sets in this study detected >20% APD_{90} decrease in response to nifedipine.

In the present study, the reduction in APD_{90} was smaller in two stimulated data sets (Cor.4U at Q-State 11% and iCell at JHU 7%), although the spontaneously beating condition at Q-State decreased APD_{90} by 22%, suggesting that overdrive stimulation (above intrinsic beat rate) reduces the observed drug-induced effect. In the Q-State Cor.4U dataset, nifedipine stopped cardiomyocyte beating at the 3 highest test concentrations, indicating prominent ion channel inhibition. Interestingly, APs could not be elicited by electrical stimulation for data

collection in these conditions, a putative advantage of employing stimulation techniques. In this study, all spontaneously beating data sets detected I_{Kr} and I_{CaL} inhibition effects with >20% change in APD_{90}.

For future studies, an even more standardized protocol can help to improve consistency and reproducibility among test sites. This includes plating condition, compound addition format, fluorescent reporter, assay solution composition, and data acquisition specifications. Considerations in experimental design choice, and recommendations for standardization of several of these assay conditions are described in Table 6. The CiPA MEA cross-platform study utilized serum containing media, and 10× compound addition solution (Millard, et al., 2018). A larger CiPA study tested 28 compounds in two cell types, with ≥5 replicates and without electrical/optical pacing, utilizing serum-containing media at sites using MEAs and serum-free media by the one VSO site, and single (in 10× solution) or cumulative (in 50× solution) dosing (Blinova, et al., 2018). Despite the methodological variation within and across these studies, in general the studies demonstrate the utility of hSC-CMs in assessment of cardiac safety of drugs.

Other electrophysiological parameters not encompassed by the CiPA initiative include calcium transient assays (alone or simultaneously with action potential) for assessing proarrhythmic risk liability (Bedut, et al., 2016; Pfeiffer, et al., 2016), which can also provide greater insight into proarrhythmia mechanisms involving calcium cycling. Optical mapping of wavefront propagation and conduction (Bursac & Tung, 2006; Entcheva & Bien, 2006; Herron, Lee, & Jalife, 2012; Lyon, et al., 2014; Pfeiffer, et al., 2014) in cell monolayers or tissues enable the characterization of arrhythmia events that involve conduction block and reentry, which are steps closer to the phenomenon of Torsade de Pointes than single cell arrhythmia events. Test protocols can be designed to detect forms of arrhythmia not examined by CiPA, including delayed after depolarizations brought about at high beat rates.

Mixed ion channel effects may play a role in defining proarrhythmic risk of drugs. These can affect repolarization to varying degrees, depending on the extent that changes in inward and outward channel currents offset each other. Recently, ECG recordings have shown that drugs that have predominantly hERG block as opposed to a balanced ion channel effect can be distinguished by measuring the time from J-wave to peak of the T-wave (J-Tpeak), and the time from peak of the T-wave to its end (Tpeak – Tend) (Johannesen, et al., 2014) in the ECG, a component of CiPA (Vicente, Zusterzeel, Johannesen, Mason, et al., 2018; Vicente, Zusterzeel, Johannesen, Ochoa-Jimenez, et al., 2018). More complete/comprehensive assessment of drug effects are possible with VSO approaches (but not with ECG or MEA recordings), in which detailed analysis of the action potential may reveal changes in multiple channel activity during all of its phases. Furthermore, features of the action potential may correspond to some extent with ECG biomarkers. For example, in transmural ECGs of the canine left ventricular wedge preparation, the J-wave occurs during the early notch of the epicardial action potential (Yan & Antzelevitch, 1996), while Tpeak occurs close to the time of maximum positive curvature and end of epicardial repolarization (Yan & Antzelevitch, 1998). This additional in vitro information, coupled with ECG-based assessments relying on J-Tpeak, could provide greater value than either approach considered alone in discriminating safe vs. unsafe repolarization changes within CiPA and outside of the ionic current/in silico reconstructions efforts that provide a proarrhthymic risk score. In this way, both VSO recordings and ECG biomarkers are useful to check for missed or unanticipated repolarization effects not necessarily detected on the basis of cardiac ionic current studies.

In summary, despite variances in protocol and acquisition method, the results of this study were relatively consistent across sites. The variety of methods selected here is representative of "real world" practice, and the consistency across sites speaks to the viability

of these methods. Overall, this cross-site study demonstrated that VSO technology is a useful *in vitro* tool for assessing pro-arrhythmia risk using hSC-CMs.

Conflict of Interest Statement

The following co-authors are employed by or have declared interests in VSO platform manufacturer companies: G.L.S., M.P.H.-V. and V.Z., Clyde Biosciences Ltd.; E.P.-K., B.C., and S.F., formerly Vala Sciences Inc; R. I., Vala Sciences Inc; and G.T.D. and C.N., Q-State Biosciences Ltd. G.A.G. is an employee of and a shareholder in the biopharmaceutical company AbbVie. R.Z., V.H. and L.T. have no conflicts to declare.

B.C.	Beibei Cai
C.N.	Cuong Nguyen
E.P.-K.	Emily R. Pfeiffer-Kaushik
G.A.G.	Gary A. Gintant
G.L.S.	Godfrey L. Smith
G.T.D.	Graham T. Dempsey
J.P.	Jennifer Pierson
L.T.	Leslie Tung
M.P.H.-V.	Maria P. Hortigon-Vinagre
R.I.	Randall Ingermanson
R.Z.	Renjun Zhu
S.F.	Shuyan Feng
V.H.	Venkatesh Hariharan
V.Z.	Victor Zamora

Acknowledgements

The Authors would like to acknowledge the HESI Cardiac Safety Committee Myocyte Subteam for their intellectual contributions to this study. Compounds were prepared and distributed by Liang Guo, Alexander Martinkosky and Doug Smallwood (Chemotherapeutic Agents Repository, National Cancer Institute, U.S. Health and Human Services). M.P.H.-V. and V.Z. were recipients of a postdoctoral fellowship from Fundacion Alfonso Martin Escudero, Spain. V.H. was a recipient of NIH postdoctoral fellowship F32 HL128079.

HESI's scientific initiatives are primarily supported by the in-kind contributions (from public and private sector participants) of time, expertise, and experimental effort, including the cells provided by Cellular Dynamics International and Axiogenesis (now Ncardia). The authors thank Ross Whittaker, Patrick McDonough and Jeffrey Price for discussion and support (Vala Sciences). These contributions are supplemented by direct funding (that primarily support program infrastructure and management) provided by HESI's corporate sponsors. This project was principally supported through in-kind contributions from the participating organizations. In addition, this research was supported in part by the Developmental Therapeutics Program in the Division of Cancer Treatment and Diagnosis of the National Cancer Institute. Also, this project has been funded in part with federal funds from the National Cancer Institute, National Institutes of Health, under contract no. HHSN261200800001E and R24 HL117756.

References

Ando, H., Yoshinaga, T., Yamamoto, W., Asakura, K., Uda, T., Taniguchi, T., Ojima, A., Shinkyo, R., Kikuchi, K., Osada, T., Hayashi, S., Kasai, C., Miyamoto, N., Tashibu, H., Yamazaki, D., Sugiyama, A., Kanda, Y., Sawada, K., & Sekino, Y. (2017). A new paradigm for drug-induced torsadogenic risk assessment using human iPS cell-derived cardiomyocytes. *J Pharmacol Toxicol Methods, 84*, 111-127.

Asakura, K., Hayashi, S., Ojima, A., Taniguchi, T., Miyamoto, N., Nakamori, C., Nagasawa, C., Kitamura, T., Osada, T., Honda, Y., Kasai, C., Ando, H., Kanda, Y., Sekino, Y., & Sawada, K. (2015). Improvement of acquisition and analysis methods in multi-electrode array experiments with iPS cell-derived cardiomyocytes. *J Pharmacol Toxicol Methods, 75*, 17-26.

Bedut, S., Seminatore-Nole, C., Lamamy, V., Caignard, S., Boutin, J. A., Nosjean, O., Stephan, J. P., & Coge, F. (2016). High-throughput drug profiling with voltage- and calcium-sensitive fluorescent probes in human iPSC-derived cardiomyocytes. *Am J Physiol Heart Circ Physiol, 311*, H44-53.

Beken, S., Kasper, P., & van der Laan, J. W. (2016). Regulatory Acceptance of Alternative Methods in the Development and Approval of Pharmaceuticals. *Adv Exp Med Biol, 856*, 33-64.

Bett, G. C., Kaplan, A. D., Lis, A., Cimato, T. R., Tzanakakis, E. S., Zhou, Q., Morales, M. J., & Rasmusson, R. L. (2013). Electronic "expression" of the inward rectifier in cardiocytes derived from human-induced pluripotent stem cells. *Heart Rhythm, 10*, 1903-1910.

Blazeski, A., Lowenthal, J., Wang, Y., Teuben, R., Zhu, R., Gerecht, S., Tomaselli, G., & Tung, L. (2018). Engineered Heart Slice Model of Arrhythmogenic Cardiomyopathy using Plakophilin-2 Mutant Myocytes. *Tissue Eng Part A*.

Blazeski, A., Zhu, R., Hunter, D. W., Weinberg, S. H., Zambidis, E. T., & Tung, L. (2012). Cardiomyocytes derived from human induced pluripotent stem cells as models for normal and diseased cardiac electrophysiology and contractility. *Prog Biophys Mol Biol, 110*, 166-177.

Blinova, K., Dang, Q., Millard, D., Smith, G., Pierson, J., Guo, L., Brock, M., Lu, H. R., Kraushaar, U., Zeng, H., Shi, H., Zhang, X., Sawada, K., Osada, T., Kanda, Y., Sekino, Y., Pang, L., Feaster, T. K., Kettenhofen, R., Stockbridge, N., Strauss, D. G., & Gintant, G. (2018). International Multisite Study of Human-Induced Pluripotent Stem Cell-Derived Cardiomyocytes for Drug Proarrhythmic Potential Assessment. *Cell Rep, 24*, 3582-3592.

Blinova, K., Stohlman, J., Vicente, J., Chan, D., Johannesen, L., Hortigon-Vinagre, M. P., Zamora, V., Smith, G., Crumb, W. J., Pang, L., Lyn-Cook, B., Ross, J., Brock, M., Chvatal, S., Millard, D., Galeotti, L., Stockbridge, N., & Strauss, D. G. (2017). Comprehensive Translational Assessment of Human-Induced Pluripotent Stem Cell Derived Cardiomyocytes for Evaluating Drug-Induced Arrhythmias. *Toxicol Sci, 155*, 234-247.

Bursac, N., & Tung, L. (2006). Acceleration of functional reentry by rapid pacing in anisotropic cardiac monolayers: formation of multi-wave functional reentries. *Cardiovasc Res, 69*, 381-390.

Casini, S., Verkerk, A. O., & Remme, C. A. (2017). Human iPSC-Derived Cardiomyocytes for Investigation of Disease Mechanisms and Therapeutic Strategies in Inherited Arrhythmia Syndromes: Strengths and Limitations. *Cardiovasc Drugs Ther, 31*, 325-344.

Cerignoli, F., Charlot, D., Whittaker, R., Ingermanson, R., Gehalot, P., Savchenko, A., Gallacher, D. J., Towart, R., Price, J. H., McDonough, P. M., & Mercola, M. (2012). High throughput measurement of Ca(2)(+) dynamics for drug risk assessment in human stem cell-derived cardiomyocytes by kinetic image cytometry. *J Pharmacol Toxicol Methods, 66*, 246-256.

Colatsky, T., Fermini, B., Gintant, G., Pierson, J. B., Sager, P., Sekino, Y., Strauss, D. G., & Stockbridge, N. (2016). The Comprehensive in Vitro Proarrhythmia Assay (CiPA) initiative - Update on progress. *J Pharmacol Toxicol Methods, 81*, 15-20.

Dempsey, G. T., Chaudhary, K. W., Atwater, N., Nguyen, C., Brown, B. S., McNeish, J. D., Cohen, A. E., & Kralj, J. M. (2016). Cardiotoxicity screening with simultaneous optogenetic pacing, voltage imaging and calcium imaging. *J Pharmacol Toxicol Methods, 81*, 240-250.

Entcheva, E., & Bien, H. (2006). Macroscopic optical mapping of excitation in cardiac cell networks with ultra-high spatiotemporal resolution. *Prog Biophys Mol Biol, 92*, 232-257.

Fermini, B., Coyne, S. T., & Coyne, K. P. (2018). Clinical Trials in a Dish: A Perspective on the Coming Revolution in Drug Development. *SLAS Discov*, 2472555218775028.

Fermini, B., Hancox, J. C., Abi-Gerges, N., Bridgland-Taylor, M., Chaudhary, K. W., Colatsky, T., Correll, K., Crumb, W., Damiano, B., Erdemli, G., Gintant, G., Imredy, J., Koerner, J., Kramer, J., Levesque, P., Li, Z., Lindqvist, A., Obejero-Paz, C. A., Rampe, D., Sawada, K., Strauss, D. G., & Vandenberg, J. I. (2016). A New Perspective in the Field of Cardiac Safety Testing through the Comprehensive In Vitro Proarrhythmia Assay Paradigm. *J Biomol Screen, 21*, 1-11.

Gintant, G. (2011). An evaluation of hERG current assay performance: Translating preclinical safety studies to clinical QT prolongation. *Pharmacol Ther, 129*, 109-119.

Gossmann, M., Frotscher, R., Linder, P., Neumann, S., Bayer, R., Epple, M., Staat, M., Artmann, A. T., & Artmann, G. M. (2016). Mechano-Pharmacological Characterization of Cardiomyocytes Derived from Human Induced Pluripotent Stem Cells. *Cell Physiol Biochem, 38*, 1182-1198.

Guo, L., Abrams, R. M., Babiarz, J. E., Cohen, J. D., Kameoka, S., Sanders, M. J., Chiao, E., & Kolaja, K. L. (2011). Estimating the risk of drug-induced proarrhythmia using human induced pluripotent stem cell-derived cardiomyocytes. *Toxicol Sci, 123*, 281-289.

Guo, L., Coyle, L., Abrams, R. M., Kemper, R., Chiao, E. T., & Kolaja, K. L. (2013). Refining the human iPSC-cardiomyocyte arrhythmic risk assessment model. *Toxicol Sci, 136*, 581-594.

Herron, T. J., Lee, P., & Jalife, J. (2012). Optical imaging of voltage and calcium in cardiac cells & tissues. *Circ Res, 110*, 609-623.

Hochbaum, D. R., Zhao, Y., Farhi, S. L., Klapoetke, N., Werley, C. A., Kapoor, V., Zou, P., Kralj, J. M., Maclaurin, D., Smedemark-Margulies, N., Saulnier, J. L., Boulting, G. L., Straub, C., Cho, Y. K., Melkonian, M., Wong, G. K., Harrison, D. J., Murthy, V. N., Sabatini, B. L., Boyden, E. S., Campbell, R. E., & Cohen, A. E. (2014). All-optical electrophysiology in mammalian neurons using engineered microbial rhodopsins. *Nat Methods, 11*, 825-833.

Honda, M., Kiyokawa, J., Tabo, M., & Inoue, T. (2011). Electrophysiological characterization of cardiomyocytes derived from human induced pluripotent stem cells. *J Pharmacol Sci, 117*, 149-159.

Hondeghem, L. M. (2008). Use and abuse of QT and TRIaD in cardiac safety research: importance of study design and conduct. *Eur J Pharmacol, 584*, 1-9.

Hondeghem, L. M., Carlsson, L., & Duker, G. (2001). Instability and triangulation of the action potential predict serious proarrhythmia, but action potential duration prolongation is antiarrhythmic. *Circulation, 103*, 2004-2013.

ICH_Expert_Working_Group. (2005). S7B The Nonclinical Evaluation of the Potential for Delayed Ventricular Repolarization (QT Interval Prolongation) by Human Pharmaceuticals. In.

Johannesen, L., Vicente, J., Mason, J. W., Sanabria, C., Waite-Labott, K., Hong, M., Guo, P., Lin, J., Sorensen, J. S., Galeotti, L., Florian, J., Ugander, M., Stockbridge, N., & Strauss, D. G. (2014). Differentiating drug-induced multichannel block on the electrocardiogram: randomized study of dofetilide, quinidine, ranolazine, and verapamil. *Clin Pharmacol Ther, 96*, 549-558.

Jonsson, M. K., Vos, M. A., Mirams, G. R., Duker, G., Sartipy, P., de Boer, T. P., & van Veen, T. A. (2012). Application of human stem cell-derived cardiomyocytes in safety pharmacology requires caution beyond hERG. *J Mol Cell Cardiol, 52*, 998-1008.

Jost, N., Virag, L., Comtois, P., Ordog, B., Szuts, V., Seprenyi, G., Bitay, M., Kohajda, Z., Koncz, I., Nagy, N., Szel, T., Magyar, J., Kovacs, M., Puskas, L. G., Lengyel, C., Wettwer, E., Ravens, U., Nanasi, P. P., Papp, J. G., Varro, A., & Nattel, S. (2013). Ionic mechanisms limiting cardiac repolarization reserve in humans compared to dogs. *J Physiol, 591*, 4189-4206.

Kitaguchi, T., Moriyama, Y., Taniguchi, T., Maeda, S., Ando, H., Uda, T., Otabe, K., Oguchi, M., Shimizu, S., Saito, H., Toratani, A., Asayama, M., Yamamoto, W., Matsumoto, E., Saji, D., Ohnaka, H., & Miyamoto, N. (2017). CSAHi study: Detection of drug-induced ion channel/receptor responses, QT prolongation, and arrhythmia using multi-electrode arrays in combination with human induced pluripotent stem cell-derived cardiomyocytes. *J Pharmacol Toxicol Methods, 85*, 73-81.

Klimas, A., Ambrosi, C. M., Yu, J., Williams, J. C., Bien, H., & Entcheva, E. (2016). OptoDyCE as an automated system for high-throughput all-optical dynamic cardiac electrophysiology. *Nat Commun, 7*, 11542.

Kramer, J., Obejero-Paz, C. A., Myatt, G., Kuryshev, Y. A., Bruening-Wright, A., Verducci, J. S., & Brown, A. M. (2013). MICE models: superior to the HERG model in predicting Torsade de Pointes. *Sci Rep, 3*, 2100.

Leyton-Mange, J. S., Mills, R. W., Macri, V. S., Jang, M. Y., Butte, F. N., Ellinor, P. T., & Milan, D. J. (2014). Rapid cellular phenotyping of human pluripotent stem cell-derived cardiomyocytes using a genetically encoded fluorescent voltage sensor. *Stem Cell Reports, 2*, 163-170.

Loew, L. M., Cohen, L. B., Dix, J., Fluhler, E. N., Montana, V., Salama, G., & Wu, J. Y. (1992). A naphthyl analog of the aminostyryl pyridinium class of potentiometric membrane dyes shows consistent sensitivity in a variety of tissue, cell, and model membrane preparations. *J Membr Biol, 130*, 1-10.

Lu, H. R., Hortigon-Vinagre, M. P., Zamora, V., Kopljar, I., De Bondt, A., Gallacher, D. J., & Smith, G. (2017). Application of optical action potentials in human induced pluripotent stem cells-derived cardiomyocytes to predict drug-induced cardiac arrhythmias. *J Pharmacol Toxicol Methods*.

Lu, H. R., Whittaker, R., Price, J. H., Vega, R., Pfeiffer, E. R., Cerignoli, F., Towart, R., & Gallacher, D. J. (2015). High Throughput Measurement of Ca++ Dynamics in Human Stem Cell-Derived Cardiomyocytes by Kinetic Image Cytometry: A Cardiac Risk Assessment Characterization Using a Large Panel of Cardioactive and Inactive Compounds. *Toxicol Sci, 148*, 503-516.

Lyon, R. C., Mezzano, V., Wright, A. T., Pfeiffer, E., Chuang, J., Banares, K., Castaneda, A., Ouyang, K., Cui, L., Contu, R., Gu, Y., Evans, S. M., Omens, J. H., Peterson, K. L., McCulloch, A. D., & Sheikh, F. (2014). Connexin defects underlie arrhythmogenic right ventricular cardiomyopathy in a novel mouse model. *Hum Mol Genet, 23*, 1134-1150.

Ma, J., Guo, L., Fiene, S. J., Anson, B. D., Thomson, J. A., Kamp, T. J., Kolaja, K. L., Swanson, B. J., & January, C. T. (2011). High purity human-induced pluripotent stem cell-derived cardiomyocytes: electrophysiological properties of action potentials and ionic currents. *Am J Physiol Heart Circ Physiol, 301*, H2006-2017.

Millard, D., Dang, Q., Shi, H., Zhang, X., Strock, C., Kraushaar, U., Zeng, H., Levesque, P., Lu, H. R., Guillon, J. M., Wu, J. C., Li, Y., Luerman, G., Anson, B., Guo, L., Clements, M., Abassi, Y. A., Ross, J., Pierson, J., & Gintant, G. (2018). Cross-Site Reliability of Human Induced Pluripotent stem cell-derived Cardiomyocyte Based Safety Assays Using Microelectrode Arrays: Results from a Blinded CiPA Pilot Study. *Toxicol Sci, 164*, 550-562.

Miller, E. W., Lin, J. Y., Frady, E. P., Steinbach, P. A., Kristan, W. B., Jr., & Tsien, R. Y. (2012). Optically monitoring voltage in neurons by photo-induced electron transfer through molecular wires. *Proc Natl Acad Sci U S A, 109*, 2114-2119.

Nunes, S. S., Miklas, J. W., Liu, J., Aschar-Sobbi, R., Xiao, Y., Zhang, B., Jiang, J., Masse, S., Gagliardi, M., Hsieh, A., Thavandiran, N., Laflamme, M. A., Nanthakumar, K., Gross, G. J., Backx, P. H., Keller, G., & Radisic, M. (2013). Biowire: a platform for maturation of human pluripotent stem cell-derived cardiomyocytes. *Nat Methods, 10*, 781-787.

Park, E., Gintant, G. A., Bi, D., Kozeli, D., Pettit, S. D., Pierson, J. B., Skinner, M., Willard, J., Wisialowski, T., Koerner, J., & Valentin, J. P. (2018). Can non-clinical repolarization assays predict the results of clinical thorough QT studies? Results from a research consortium. *Br J Pharmacol, 175*, 606-617.

Passini, E., Britton, O. J., Lu, H. R., Rohrbacher, J., Hermans, A. N., Gallacher, D. J., Greig, R. J. H., Bueno-Orovio, A., & Rodriguez, B. (2017). Human In Silico Drug Trials Demonstrate Higher Accuracy than Animal Models in Predicting Clinical Pro-Arrhythmic Cardiotoxicity. *Front Physiol, 8*, 668.

Peng, S., Lacerda, A. E., Kirsch, G. E., Brown, A. M., & Bruening-Wright, A. (2010). The action potential and comparative pharmacology of stem cell-derived human cardiomyocytes. *J Pharmacol Toxicol Methods, 61*, 277-286.

Pfeiffer, E. R., Vega, R., McDonough, P. M., Price, J. H., & Whittaker, R. (2016). Specific prediction of clinical QT prolongation by kinetic image cytometry in human stem cell derived cardiomyocytes. *J Pharmacol Toxicol Methods, 81*, 263-273.

Pfeiffer, E. R., Whittaker, R., Vega, R., Cerignoli, F., McDonough, P. M., & Price, J. H. (2017). Kinetic Image Cytometry for Predicting Arrhythmias Using Human Stem Cell-Derived Cardiomyocytes. In M. Clements & L. Roquemore (Eds.), *Stem Cell-Derived Models in Toxicology* (pp. 153-171). New York: Springer Science+Business Media.

Pfeiffer, E. R., Wright, A. T., Edwards, A. G., Stowe, J. C., McNall, K., Tan, J., Niesman, I., Patel, H. H., Roth, D. M., Omens, J. H., & McCulloch, A. D. (2014). Caveolae in ventricular myocytes are required for stretch-dependent conduction slowing. *J Mol Cell Cardiol, 76*, 265-274.

Piccini, I., Rao, J., Seebohm, G., & Greber, B. (2015). Human pluripotent stem cell-derived cardiomyocytes: Genome-wide expression profiling of long-term in vitro maturation in comparison to human heart tissue. *Genom Data, 4*, 69-72.

Pierson, J. B., Berridge, B. R., Brooks, M. B., Dreher, K., Koerner, J., Schultze, A. E., Sarazan, R. D., Valentin, J. P., Vargas, H. M., & Pettit, S. D. (2013). A public-private consortium advances cardiac safety evaluation: achievements of the HESI Cardiac Safety Technical Committee. *J Pharmacol Toxicol Methods, 68*, 7-12.

Puppala, D., Collis, L. P., Sun, S. Z., Bonato, V., Chen, X., Anson, B., Pletcher, M., Fermini, B., & Engle, S. J. (2013). Comparative gene expression profiling in human-induced pluripotent stem cell--derived cardiocytes and human and cynomolgus heart tissue. *Toxicol Sci, 131*, 292-301.

Rajamohan, D., Kalra, S., Duc Hoang, M., George, V., Staniforth, A., Russell, H., Yang, X., & Denning, C. (2016). Automated electrophysiological and pharmacological evaluation of human pluripotent stem cell-derived cardiomyocytes. *Stem Cells Dev, 25*, 439-452.

Redfern, W. S., Carlsson, L., Davis, A. S., Lynch, W. G., MacKenzie, I., Palethorpe, S., Siegl, P. K., Strang, I., Sullivan, A. T., Wallis, R., Camm, A. J., & Hammond, T. G. (2003). Relationships between preclinical cardiac electrophysiology, clinical QT interval prolongation and torsade de pointes for a broad range of drugs: evidence for a provisional safety margin in drug development. *Cardiovasc Res, 58*, 32-45.

Sager, P. T., Gintant, G., Turner, J. R., Pettit, S., & Stockbridge, N. (2014). Rechanneling the cardiac proarrhythmia safety paradigm: a meeting report from the Cardiac Safety Research Consortium. *Am Heart J, 167*, 292-300.

Sanguinetti, M. C., Jiang, C., Curran, M. E., & Keating, M. T. (1995). A mechanistic link between an inherited and an acquird cardiac arrthytmia: HERG encodes the IKr potassium channel. *Cell, 81*, 299-307.

Sayed, N., Liu, C., & Wu, J. C. (2016). Translation of Human-Induced Pluripotent Stem Cells: From Clinical Trial in a Dish to Precision Medicine. *J Am Coll Cardiol, 67*, 2161-2176.

Scheel, O., Frech, S., Amuzescu, B., Eisfeld, J., Lin, K. H., & Knott, T. (2014). Action potential characterization of human induced pluripotent stem cell-derived cardiomyocytes using automated patch-clamp technology. *Assay Drug Dev Technol, 12*, 457-469.

Scott, C. W., Zhang, X., Abi-Gerges, N., Lamore, S. D., Abassi, Y. A., & Peters, M. F. (2014). An impedance-based cellular assay using human iPSC-derived cardiomyocytes to quantify modulators of cardiac contractility. *Toxicol Sci, 142*, 331-338.

Shadrin, I. Y., Allen, B. W., Qian, Y., Jackman, C. P., Carlson, A. L., Juhas, M. E., & Bursac, N. (2017). Cardiopatch platform enables maturation and scale-up of human pluripotent stem cell-derived engineered heart tissues. *Nat Commun, 8*, 1825.

Shinnawi, R., Huber, I., Maizels, L., Shaheen, N., Gepstein, A., Arbel, G., Tijsen, A. J., & Gepstein, L. (2015). Monitoring Human-Induced Pluripotent Stem Cell-Derived Cardiomyocytes with Genetically Encoded Calcium and Voltage Fluorescent Reporters. *Stem Cell Reports, 5*, 582-596.

Shinozawa, T., Nakamura, K., Shoji, M., Morita, M., Kimura, M., Furukawa, H., Ueda, H., Shiramoto, M., Matsuguma, K., Kaji, Y., Ikushima, I., Yono, M., Liou, S. Y., Nagai, H., Nakanishi, A., Yamamoto, K., & Izumo, S. (2017). Recapitulation of Clinical Individual Susceptibility to Drug-Induced QT Prolongation in Healthy Subjects Using iPSC-Derived Cardiomyocytes. *Stem Cell Reports, 8*, 226-234.

Sirenko, O., Cromwell, E. F., Crittenden, C., Wignall, J. A., Wright, F. A., & Rusyn, I. (2013). Assessment of beating parameters in human induced pluripotent stem cells enables quantitative in vitro screening for cardiotoxicity. *Toxicol Appl Pharmacol, 273*, 500-507.

Sun, X., & Nunes, S. S. (2016). Biowire platform for maturation of human pluripotent stem cell-derived cardiomyocytes. *Methods, 101*, 21-26.

Tertoolen, L. G. J., Braam, S. R., van Meer, B. J., Passier, R., & Mummery, C. L. (2018). Interpretation of field potentials measured on a multi electrode array in pharmacological toxicity screening on primary and human pluripotent stem cell-derived cardiomyocytes. *Biochem Biophys Res Commun, 497*, 1135-1141.

Tornqvist, E., Annas, A., Granath, B., Jalkesten, E., Cotgreave, I., & Oberg, M. (2014). Strategic focus on 3R principles reveals major reductions in the use of animals in pharmaceutical toxicity testing. *PLoS One, 9*, e101638.

Trepakova, E. S., Koerner, J., Pettit, S. D., Valentin, J. P., & Committee, H. P.-A. (2009). A HESI consortium approach to assess the human predictive value of non-clinical repolarization assays. *J Pharmacol Toxicol Methods, 60*, 45-50.

Vicente, J., Zusterzeel, R., Johannesen, L., Mason, J., Sager, P., Patel, V., Matta, M. K., Li, Z., Liu, J., Garnett, C., Stockbridge, N., Zineh, I., & Strauss, D. G. (2018). Mechanistic model-informed proarrhythmic risk assessment of drugs: review of the "CiPA" initiative and design of a prospective clinical validation study. *Clin Pharmacol Ther, 103*, 54-66.

Vicente, J., Zusterzeel, R., Johannesen, L., Ochoa-Jimenez, R., Mason, J. W., Sanabria, C., Kemp, S., Sager, P. T., Patel, V., Matta, M. K., Liu, J., Florian, J., Garnett, C., Stockbridge, N., & Strauss, D. G. (2018). Assessment of multi-ion channel block in a phase I randomized study design: results of the CiPA Phase I ECG Biomarker Validation Study. *Clin Pharmacol Ther*.

Wallis, R. M. (2010). Integrated risk assessment and predictive value to humans of non-clinical repolarization assays. *Br J Pharmacol, 159*, 115-121.

Xu, Y., Zou, P., & Cohen, A. E. (2017). Voltage imaging with genetically encoded indicators. *Curr Opin Chem Biol, 39*, 1-10.

Yan, G. X., & Antzelevitch, C. (1996). Cellular basis for the electrocardiographic J wave. *Circulation, 93*, 372-379.

Yan, G. X., & Antzelevitch, C. (1998). Cellular basis for the normal T wave and the electrocardiographic manifestations of the long-QT syndrome. *Circulation, 98*, 1928-1936.

Zeng, H., Roman, M. I., Lis, E., Lagrutta, A., & Sannajust, F. (2016). Use of FDSS/muCell imaging platform for preclinical cardiac electrophysiology safety screening of compounds in human induced pluripotent stem cell-derived cardiomyocytes. *J Pharmacol Toxicol Methods, 81*, 217-222.

Site	Optical Sensor	Sensor Kinetics for Change in Voltage	Excitation (nm)	Detector (Data Acquisition Rate [Hz])	Unit measurement area	n/ (total area per well)	Pacing/ Spontaneous	Cell Source (plating density)	Imaging Solution	Compound Addition, Treatment Duration
Clyde	di-4-ANEPPS	< 1 ms	480	PMT (10,000)	0.2 x 0.2 mm^2	1 (0.2 x 0.2 mm^2)	Spont	Cor.4U (78k/cm^2); iCell (78k/cm^2)	Cor.4U: modified BMCC; iCell: modified DMEM	Single conc. (5X), 30 minutes
JHU	di-4-ANEPPS	< 1 ms	531	CMOS (500)	0.1 x 0.1 mm^2	~7,000 (10 x10 mm^2)	Electrical	Cor.4U (160k/cm^2); iCell (255k/cm^2);	Modified Tyrode's	Cumulative (10X), 10 minutes
Q-State	QuasAr	< 3 ms	640	sCMOS (500)	0.4 x 0.4 μm^2	75,000 (3 x 0.2 x 0.2 mm^2)	Optical /Spont	Cor.4U (70k/cm^2); iCell (70k/cm^2)	Custom media	Cumulative (10X), 10 minutes
Vala	FluoVolt	< 1 ms	488	sCMOS (30)	0.325 x 0.325 μm^2	~3 million (0.58 x 0.58 mm^2)	Spont	Cor.4U (140k/cm^2); iCell (78k/cm^2)	Modified Tyrode's	Single conc. (1X), 20 minutes

Table 1. Summary of data acquisition and cell conditions used across each VSO site.

Voltage-sensitive optical sensor acquisition methods were unique per site. Unit measurement area is the area from which single measurements were taken and parameters calculated. n is the typical number of measurements made per well or monolayer. Each imaging solution is serum-free with unique composition, as described in Supplemental Table 1. Compound addition denotes the intermediate concentration (conc.) of compound added to the cells (e.g. 1×, 5×, 10× the test concentration). Refer to **Methods** for more details.

Compound	Currents Inhibited	Conc. 1 (µM)	Conc. 2 (µM)	Conc. 3 (µM)	Conc. 4 (µM)
E-4031	I_{Kr}	0.003	0.01	0.03	0.1
Nifedipine	I_{Ca}	0.01	0.03	0.1	0.3
Mexiletine	I_{Na}	1	3	10	30
JNJ 303	I_{Ks}	0.01	0.03	0.1	0.3
Flecainide	Multiple (I_{Kr}, I_{Na}, I_{to})	0.1	0.3	1	3
Moxifloxacin	I_{Kr}, I_{Ca}	3	10	30	100
Quinidine	Multiple (I_{Kr}, I_{Ca}, I_{Na}, I_f)	0.3	1	3	10
Ranolazine	Multiple (I_{Kr}, I_{NaL})	1	3	10	30

Table 2. Test compounds and dosages.

		Clyde				JHU				QState				Vala (*)			
		Cor.4U (n=192)		iCell (n=192)		Cor.4U (n=9)		iCell (n=9)		Cor.4U (n=59)		iCell (n=57)		Cor.4U (n=33)		iCell (n=36)	
		mean (SD)	CoV	mean (SD)	CoV	mean (SD)	CoV	mean (SD)	CoV	mean (SD)	CoV	mean (SD)	CoV	mean (SD)	CoV	mean (SD)	CoV
Spont	CL (s)	0.81 (0.11)	0.14	1.3 (0.3)	0.23					1.7 (1.1)	0.65	1.7 (0.3)	0.18	1.3 (0.2)	0.15	3.7 (0.4)	0.11
	APD30 (ms)	127.2 (21.8)	0.17	259 (46.2)	0.18					213.3 (63.6)	0.30	301.4 (61.7)	0.20	255.8 (32.7)	0.13	466.5 (83.1)	0.18
	APD60 (ms)	172 (19.6)	0.11	403.7 (63.5)	0.16					294.6 (91.6)	0.31	442.4 (66.5)	0.15	333.9 (32)	0.10	726 (59.8)	0.08
	APD90 (ms)	215.4 (26)	0.12	471.7 (59.9)	0.13					413.5 (102)	0.25	563 (61.2)	0.11	404.1 (32.7)	0.08	807 (58.7)	0.07
	TRise (ms)	9.9 (3)	0.30	5.9 (1.5)	0.25					25.7 (10.3)	0.40	13.7 (1.9)	0.14	36.1 (3.3)	0.09	41.6 (5.6)	0.13
	Triang (ms)	88.3 (22.4)	0.25	212.7 (57.9)	0.27					198.6 (59.3)	0.30	261.6 (26.9)	0.10	148.3 (7.7)	0.05	340.5 (57.3)	0.17
1Hz	CL (s)					1		1		1		1					
	APD30 (ms)					265.2 (12.8)	0.05	271.4 (17.7)	0.07	198.2 (49.6)	0.25	257.1 (43.3)	0.17				
	APD60 (ms)					349.1 (13.8)	0.04	380.1 (16.7)	0.04	274.5 (72.1)	0.26	372.8 (41.3)	0.11				
	APD90 (ms)					442.4 (16.1)	0.04	524.3 (24.3)	0.05	378.6 (80.9)	0.21	497.8 (36.6)	0.07				
	TRise (ms)					16.3 (2)	0.12	21.3 (2.5)	0.12	26 (9.6)	0.37	16.1 (7.8)	0.48				
	Triang (ms)					177.3 (12.9)	0.07	252.3 (22.9)	0.09	180.4 (46.8)	0.26	240.7 (25.7)	0.11				

Table 3. Measured baseline action potential parameters. Average (mean), standard deviation (SD) and coefficient of variation (CoV) of action potential parameters recorded under baseline (not test article treated) conditions. *In the presence of DMSO.

All Sites, All Data	Linear Regression	r^2
Cor.4U	Y = 0.09718*X + 197.4	0.2468
iCell	Y = 0.1286*X + 324.8	0.8117

Table 4. Dependence of APD_{90} on cycle length. Linear regression for all sites, all spontaneous or stimulated baseline data combined. X: cycle length (ms); Y: APD_{90} (ms).

Drug	µM	Clyde (n=3)		JHU (n=1)		Q-State (n=3)				Vala (n=3)	
		Cor.4U	iCell	Cor.4U	iCell	Cor.4U		iCell		Cor.4U	iCell
		Spont	Spont	1 Hz	1 Hz	Spont	1 Hz	Spont	1 Hz	Spont	Spont
E-4031	0.003										
	0.01										
	0.03	B(2) T(1)	A(2) B(1)					C (1)			A (2)
	0.1	T (3)	T (3)	B (1)		Q (3)	Q (3)	C (2)		A (3)	A (2)
Nifedipine	0.01										
	0.03					Q (3)	Q (3)				
	0.1					Q (3)	Q (3)	Q (2)			T (3)
	0.3			Q (1)		Q (3)	Q (3)	Q (3)			T (3)
Mexiletine	1										
	3										
	10							Q (2)			
	30		Q (3)					Q (3)			IrrBeat (3)
JNJ 303	0.01										
	0.03										
	0.1										
	0.3										
Flecainide	0.1										
	0.3										
	1		A (3)					Q (1)			
	3	B (3)	C(2) Q(1)					Q (2)	C (2)		A (2)
Moxifloxacin	3										
	10										
	30										
	100										
Quinidine	0.3										
	1										A (3)
	3		T (3)					A (2)			A (2)
	10		Q (3)	Q (1)	Q (1)	Q (3)	Q (2)	T (3)			A (3)
Ranolazine	1										
	3										
	10									A (2)	
	30									B,C (3)	A (1)

Table 5. Incidence of arrhythmia-like events. Events are annotated by number and type, which consist of single transient depolarizations during the plateau phase of the AP (type A),

oscillating or multiple depolarizing events during the plateau phase (type B), rapid depolarizing events during the late repolarization phase of the AP (type C), tachycardia-like with sustained high frequency spontaneous activity > 2Hz (type T), quiescent cells having no recorded AP signal for a period of the recording time (> 20s) (type Q), and irregular beat rhythmicity (extended period between two beats) (type IrrBeat). AP waveforms for different types of events are shown in **Supplemental Figure 1**.

Assay Condition	Variations (Recommendation)	Considerations
Cell type	iCell hSC-CM Cor.4U hSC-CM	Cell-type specific protocols and criteria for data interpretation should be utilized.
Cell culture duration	4 to 17 days	Cells should be maintained in culture for a sufficient time following thawing or dissociation to reduce variation in baseline characteristics.
Cell culture modifications	Dissociation, viral transfection	Minimization of cell handling steps and implementation of quality inclusion criteria for baseline variation may decrease variability in experimental results.
Beat rate control	Electrically or optically stimulated at 1 Hz, or **(spontaneously beating)**	Beat rate control is meant to avoid rate-duration dependence, but rate constraint can suppress drug-induced effects and is technically limiting.
Test article addition	Cummulative or **(single)** dosing, **(full)** or 1:10 to 1:2 media exchange	Addition of 5X-10X intermediate stock solution and cumulative dosing has greater tendency to stop spontaneous beating.
Test article exposure duration	10, **(20, 30 minutes)**	Shorter exposure accomodates repeat-dosing and increases throughput, but may limit sensitivity and be susceptible to non-equilibrium conditions
Recording rate	30 to 10,000 Hz	Higher recording rate supports finer time scale resolution. • $\geqslant$ 30 Hz for CL, APD • $\geqslant$ 500 Hz for Trise
Imaging solution	Various ionic and supplemental formulations	The constituency of assay solution and ionic composition have complex influences on cell electrophysiological properties, potentially affecting cycle length and action potential duration. These may be best examined through single factor variation.

Table 6. Recommended assay conditions. Evaluation of select assay condition variants occurring in this study and recommendations for routine use.

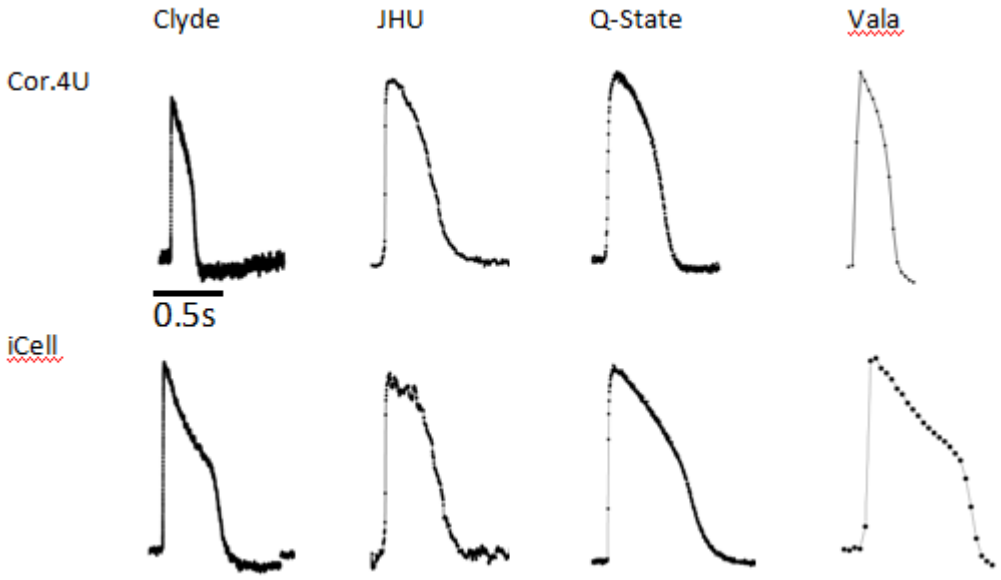

Figure 1. Baseline optical signals from voltage sensing optical sensors (VSOs). Baseline action potential signals from Cor.4U and iCell cardiomyocytes recorded using VSOs recorded at four sites (Clyde, JHU, Q-State, and Vala). Signals are shown as point/line plots with points indicating sample rate of acquisition device.

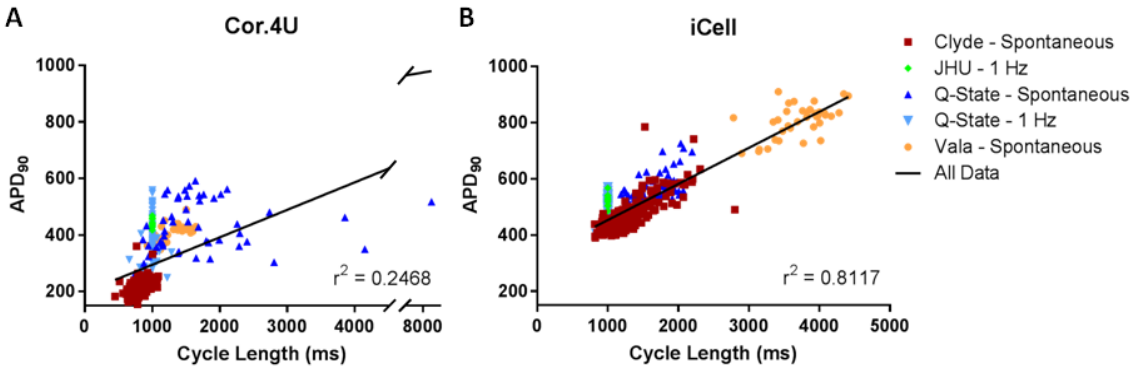

Figure 2. Relationship of APD_{90} to cycle length. APD_{90} (ms) and cycle length (ms) data in control spontaneously beating or 1Hz stimulated . (A) Cor.4U and (B) iCell cardiomyocytes. Data are fit by linear regression.

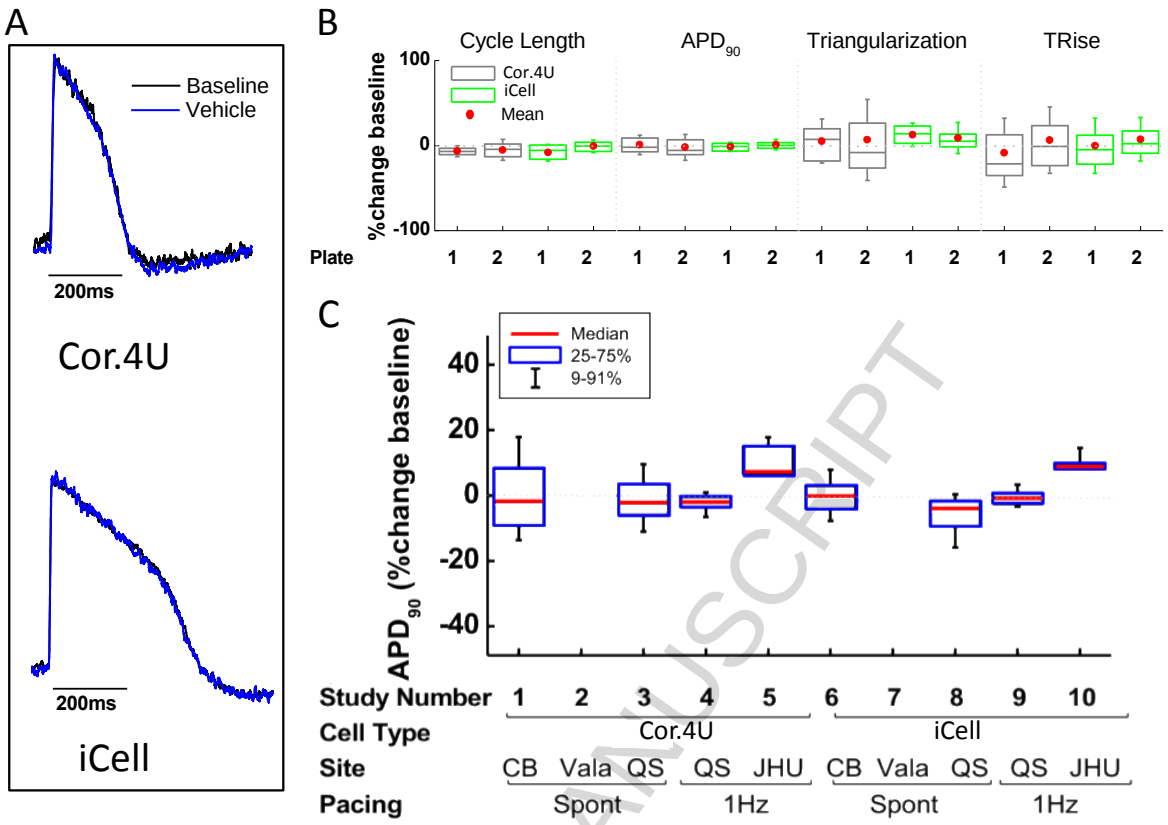

Figure 3. The effect of vehicle (DMSO) on optical action potential parameters. (A) Example AP signals from Cor.4U and iCell cardiomyocytes prior to (black) and after 30 min exposure to DMSO (blue line) as measured at one site Clyde Biosciences (CB). (B) The relative change in electrophysiological parameters across 8 plates of 96 well format measured at CB from spontaneously active cells. The values in each plate are an average of measurements from 10 wells, the boxes denote the 25% and 75% limits and the whiskers 9% and 91% limits. (C) The changes in APD_{90} due to addition of vehicle across all sites recorded from both stimulated and spontaneously active cells. The line represents median value, the box 25% to 75% limits and the whisker 9% to 91%. Note that the Vala site did not record a baseline value and only recorded in the presence of DMSO.

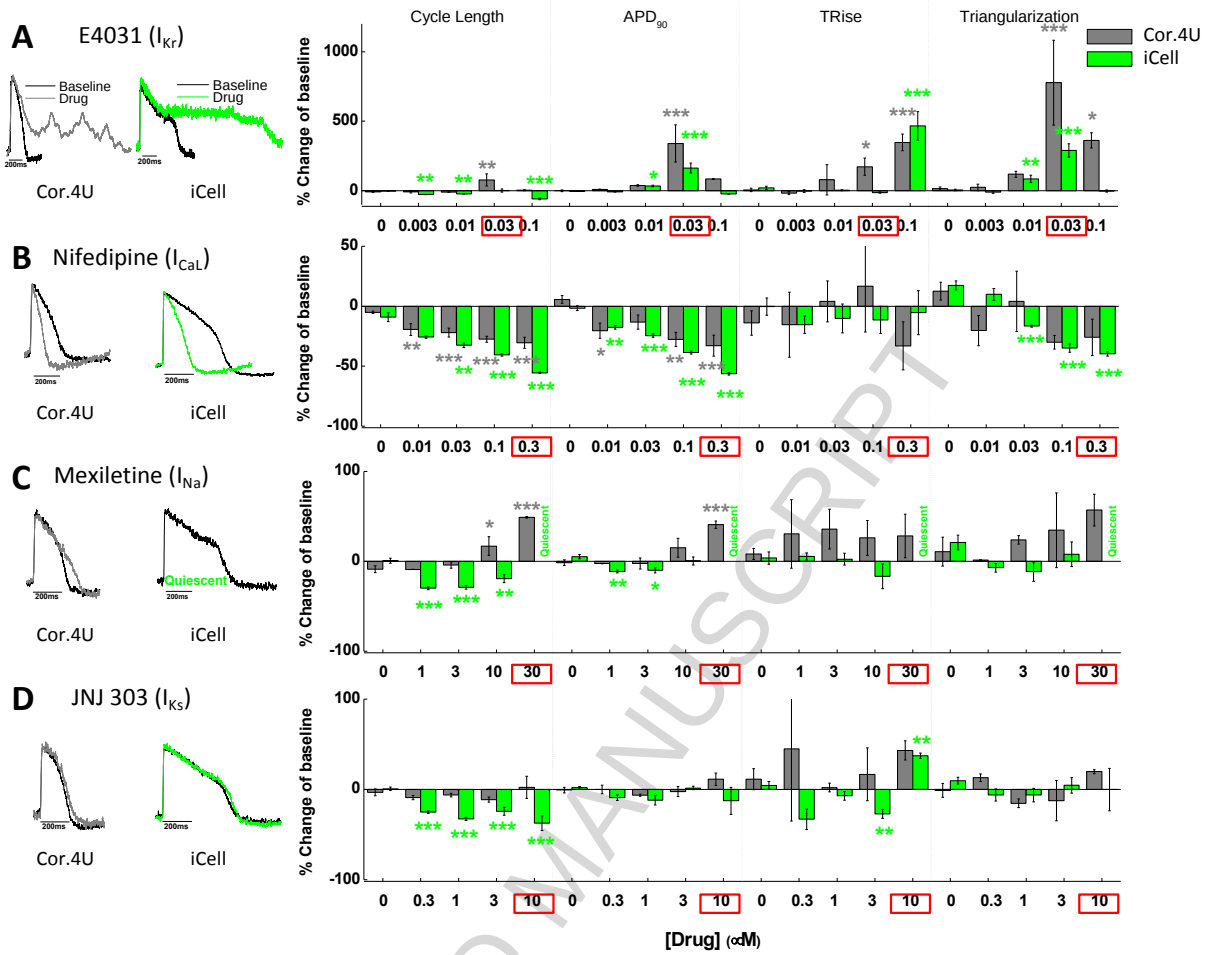

Figure 4. Electrophysiological responses to a subset of drugs from one site (CB). Response of Cor.4U and iCell cardiomyocytes to (A) E-4031, (B) nifedipine, (C) mexiletine, and (D) JNJ303. (Left) Sample records of changes in AP characteristics in response to (A) 30 nM E-4031, (B) 300 nM nifedipine, (C) 30 µM mexiletine, and (D) 10 µM JNJ 303. (Right) Changes in cycle length, APD_{90}, triangulation (APD_{90}-APD_{30}) and Trise (10 to 90% of upstroke) with addition of drug. Red boxes indicate the test concentrations of drug used in the records on the left.

A Cor.4U

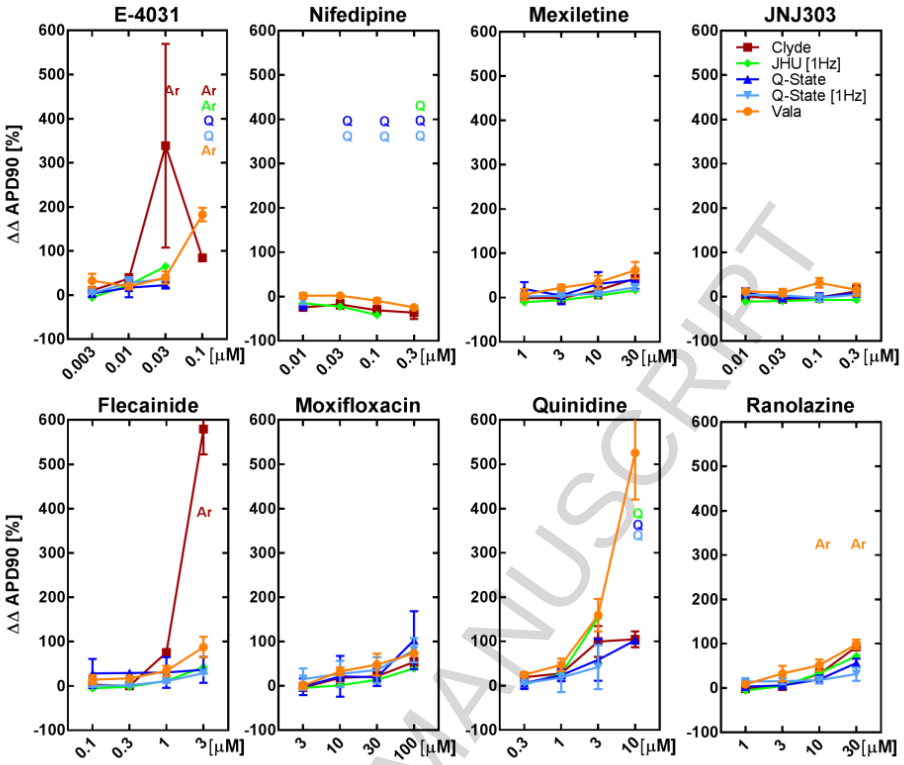

B iCell

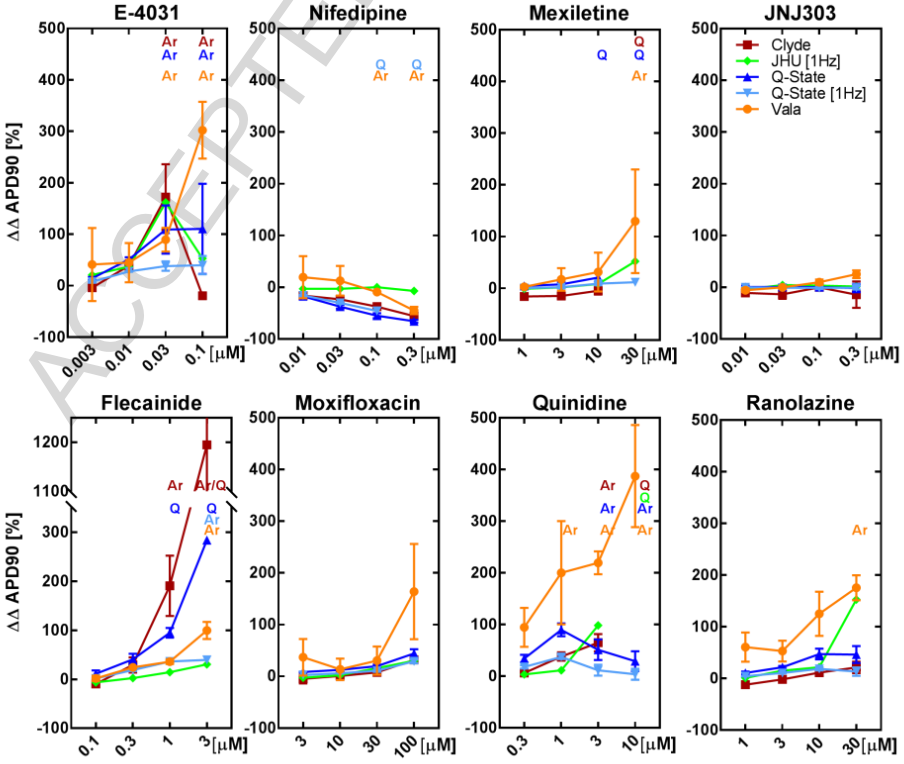

Figure 5. Change in ADP_{90} in response to a subset of drugs from all four test sites. Plots of the mean and standard error of the relative change in APD_{90} from vehicle control (DMSO) ($\Delta\Delta APD_{90}$) for the 4 sites, for (A) Cor.4U, and (B) iCell cardiomyocytes, under spontaneously beating (spont) or electrically or optically paced (1Hz) conditions. Q indicates a quiescent response (cells stopped beating), Ar denotes an arrhythmia event as detailed in **Table 5**).

SUPPLEMENTAL TABLES & FIGURES

	Extracellular Matrix Protein	Days of culture (day dissociated)	Imaging Media	Imaging Solution Ionic Composition	Imaging Solution Supplement	pH
Clyde (Cor.4U)	fibronectin (10 µg/ml)	Cor.4U: 4-8	BMCC	86.3 NaCl 4.4 KCl 1.5 $CaCl_2$ 0.81 $MgSO_4$ 0.91 NaH_2PO_4	25 glucose $7.5x10^{-4}$ KNO_3 $3.8x10^{-5}$ $Na_2SeO_3*5H_20$ 34 $NaHCO_3$	7.4
Clyde (iCell)	fibronectin (10 µg/ml)	iCell: 10-15	DMEM	110 NaCl 5.33 KCl 1.8 $CaCl_2$ 0.81 $MgSO_4$ 0.91 NaH_2PO_4	10 galactose 10 Na-pyruvate $2.5x10^{-4}$ $Fe(NO3)_3$ 44 $NaHCO_3$	7.4
JHU	Geltrex (1:100 dilution)	Cor.4U: 10 (2) iCell: 10	Tyrode's	135 NaCl 5.4 KCl 1.8 $CaCl_2$ 1.0 $MgCl_2$ 0.33 NaH_2PO_4	5 glucose 5 HEPES Cor.4U: 0.01 blebbistatin	7.4
Q-State	0.1% gelatin, 10 µg/mL fibronectin in 0.1% gelatin	Cor.4U: 7-10 iCell:14-17 (transduced at 3-5, dissociated at 6)	Custom	129 NaCl 5.3 KCl 1.8 $CaCl_2$ 0.81 $MgSO_4$ 0.91 NaH_2PO_4	10 D-(+)-galactose 1 Na-pyruvate $2.5x10^{-4}$ $Fe(NO3)_3$ 44 $NaHCO_3$	7.3
Vala	Cor.4U: fibronectin (10 µg/mL) iCell: Matrigel (250 µg/ml)	Cor.4U: 6 iCell:10	Tyrode's	135 NaCl 4.5 KCl 2.0 $CaCl_2$ 1.0 $MgCl_2$	10 glucose 25 HEPES	7.4

Supplemental Table 1. Composition of experimental solutions. Each site used the cell manufacturer-supplied plating and maintenance medias. Days of culture post-thaw are recorded, some sites dissociated and re-plated the cells during this period. All imaging solutions were serum free, composition is described in mM.

		Clyde (Spontaneous)		Q-State (Spontaneous)		Vala (Spontaneous)	
		mean	SD	mean	SD	mean	SD
Cor.4U	Intercept (ms)	128	12	373	24	265	27
	Slope	0.108	0.015	0.024	0.012	0.108	0.020
	r^2	0.2201		0.06954		0.476	
iCell	Intercept (ms)	289	12	356	37	500	81
	Slope	0.138	0.009	0.125	0.022	0.083	0.022
	r^2	0.570		0.375		0.302	

Supplemental Table 2. Linear regression of individual sites APD_{90} by cycle length (as relates to Figure 2).

Drug	Indication	FDA Approval	Credible Meds: Risk of TdP	$ETPC_{free}$ Range [μM]	$ETPC_{free}$ References	C_{max} of Clinical QTc Prolongation >10 ms [μM]	Clinical References		Concentrations Tested [μM] (First arrhythmia)
							QTc	Arrhythmia	
E-4031	experimental antiarrhythmic (class III)	-	-	0.001 – 0.021	(14,15,30)	0.003	(15)		0.003 – 0.1 (0.03 μM EAD)
Nifedipine	antihypertensive (calcium channel block)	1989	No evidence of risk	0.002 – 0.01	(22,33,40)				0.01 – 0.3 (0.03 μM Q, Tachy)
Mexiletine	antiarrhythmic (class IB)	1998	No evidence of risk	0.47 – 1.1	(19,40)				1 – 30 (10 μM Q and Irregular Beats)
JNJ 303	development compound, JNJ-38445303 I_{Ks} blocker	-	-	Not tested clinically	(39)				0.01 – 0.3 (none)
Flecainide	antiarryhthmic (class Ic)	1985	Known Risk	0.3 – 1.9	(10,25,32)	0.59 – 0.72	(2,12)	(1,9)	0.1 – 3 (1 μM EAD, Q)
Moxifloxacin	antibiotic	1999	Known Risk	0.2 – 4.8	(4,5,26,37)	2.1 – 4.1	(13,16,28,35)		3 – 100 (none)
Quinidine	antiarrhythmic (class Ia)	1950	Known Risk	0.29 – 22	(6,25,29,32)	0.064 – 2.3	(6,27,29,32,36)	(9)	0.3 – 10 (1 μM EAD, Q)
Ranolazine	antianginal	2006	Conditional Risk	0.62 – 5.2	(8,16,21,38)	3.5 – 9.1	(16,21)		1 – 30 (10 μM EAD)

Supplemental Table 3. Description and clinical usage of drugs tested. Clinical status and CredibleMeds® categorization of TdP risk (QTDrugsList at https://crediblemeds.org). Unbound effective therapeutic plasma concentration ($ETPC_{free}$) and plasma concentrations (unbound C_{max}) associated with QTc prolongation of the drugs tested in this study, coincide with the lower concentrations tested. The lowest test concentrations at which arrhythmia occurred are provided for comparison.

Compound	hERG (I_{Kr}) IC50 [μM]	*hERG reference*	Nav1.5 (I_{Na}) IC50 [μM]	*Nav1.5 reference*	Cav1.2 (I_{CaL}) IC50 [μM]	*Cav1.2 reference*	IKs IC50 [μM]	IKs *reference*	Nav1.5-Late (I_{NaL}) IC50 [μM]	*Nav1.5-Late reference*
E-4031	0.005 - 0.4	(30)								
Nifedipine	44 - 275	(23,30)	88	(23)	0.012	(23)				
Mexiletine	3.7-28.9	(18,24)	8.4 - 135	(7,11,20)	38.2	(24)			9	(24)
JNJ 303	12.6	(39)	3.3	(39)			0.064	(39)		
Flecainide	0.004 – 3.9	(7,23,30,32)	6.2 – 10.7	(7,11,20,23)	27, >20	(7,23)				
Moxifloxacin	77 – 93	(7,17,23)	1112, >350	(7,23)	173, >350	(7,23)				
Quinidine	0.3 – 1.5	(7,11,23,24,30)	12 – 46	(7,11,23,24)	6.4- 51.6, >5.4	(7,23,24)			9.4	(24)
Ranolazine	8.3 – 106	(24,31,34)	1.4 – 10	(3,7,24)	296	(3)			7.9	(24)

Supplemental Table 4. Cardiac ion channel inhibition by test compounds.

.

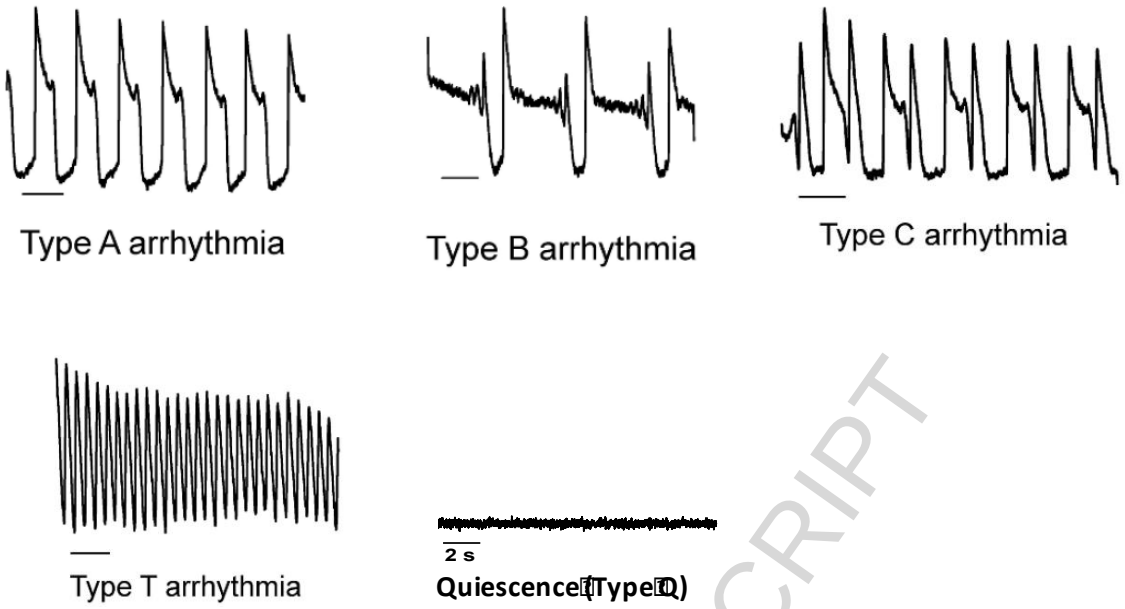

Supplemental Figure 1. Classification of "cellular arrhythmias." Exemplar records recorded from hSC-CM with distinct characteristics. Type A events are single transient depolarizations during the plateau phase of the AP. Type B events are oscillating or multiple depolarizing events during the plateau phase. Type C events are rapid depolarizing events during the late repolarization phase of the AP. Tachycardia-like events (Type T) are sustained high frequency spontaneous activity (>2Hz), and quiescent cells have no recorded AP signal for a period of the recording time (> 20s) (Type Q).

A Cycle Length

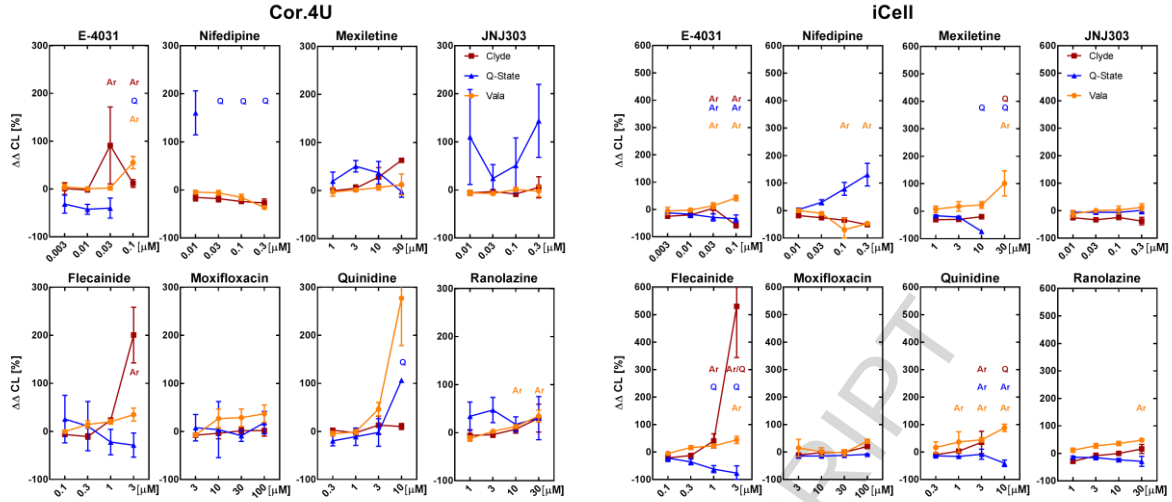

B APD_{30}

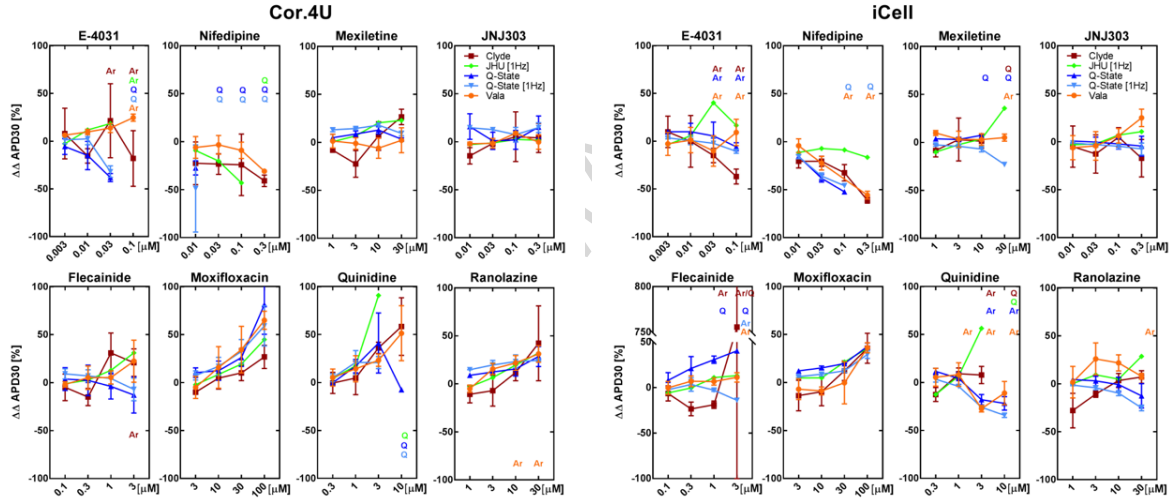

C APD_{60}

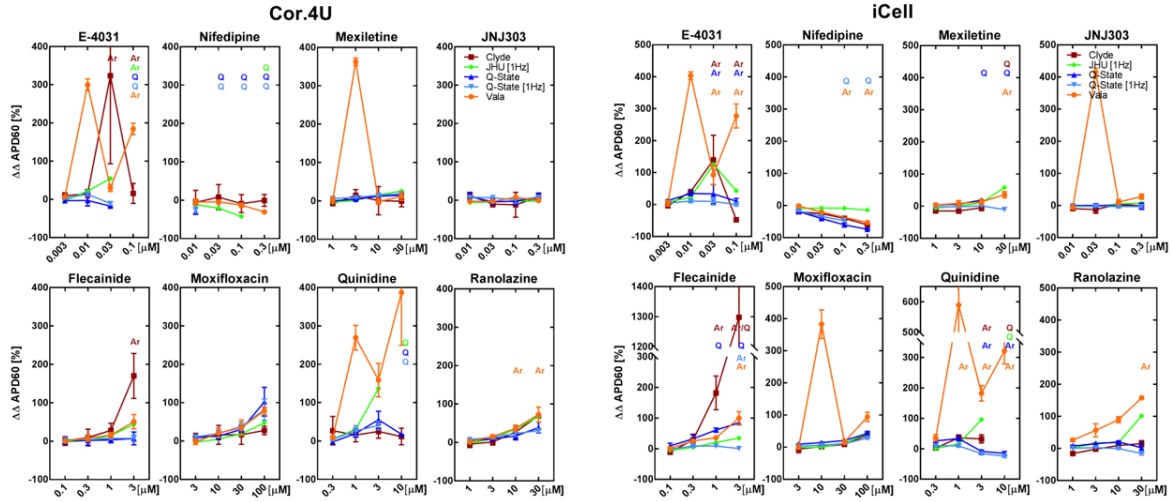

D APD_{90}

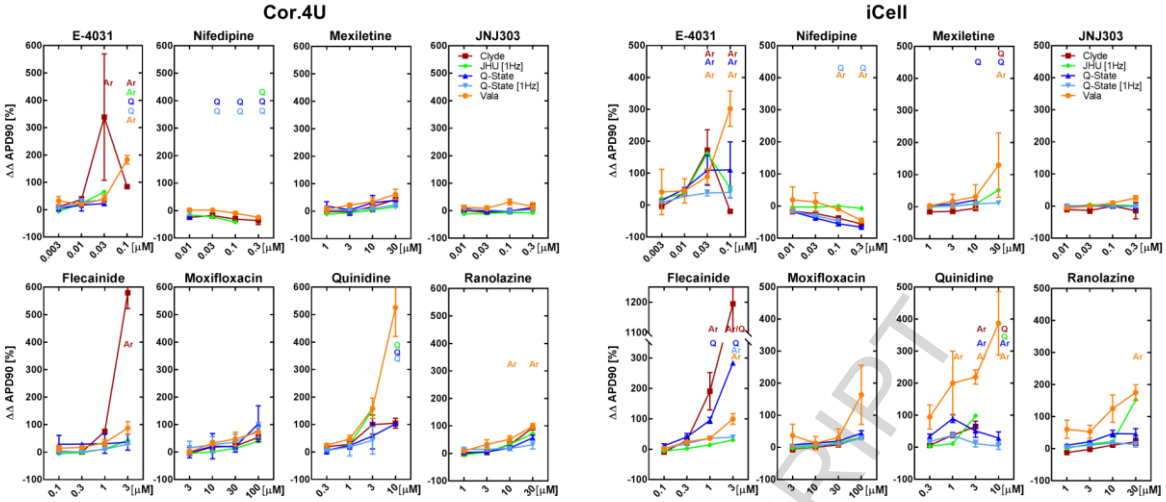

E TRise

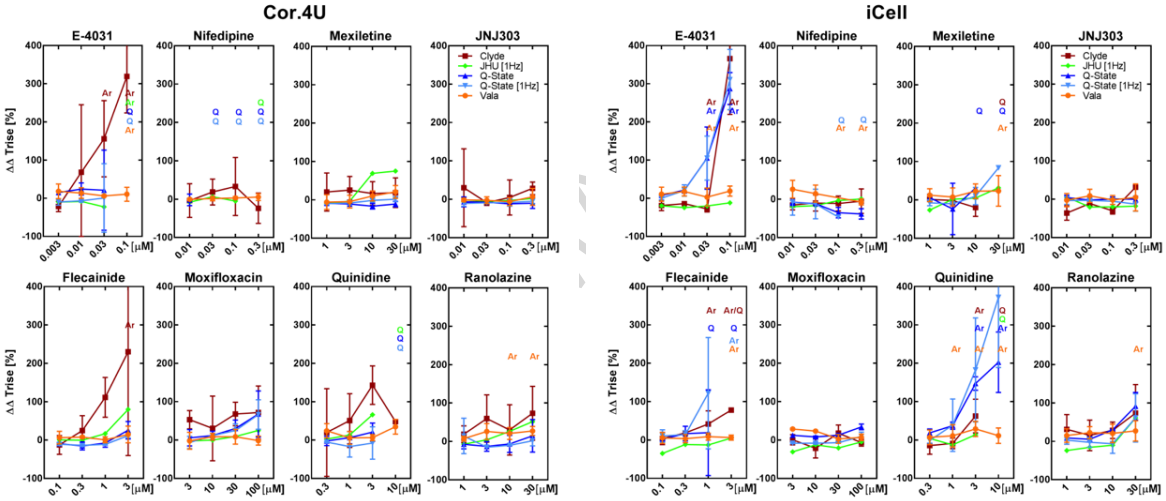

F Triang

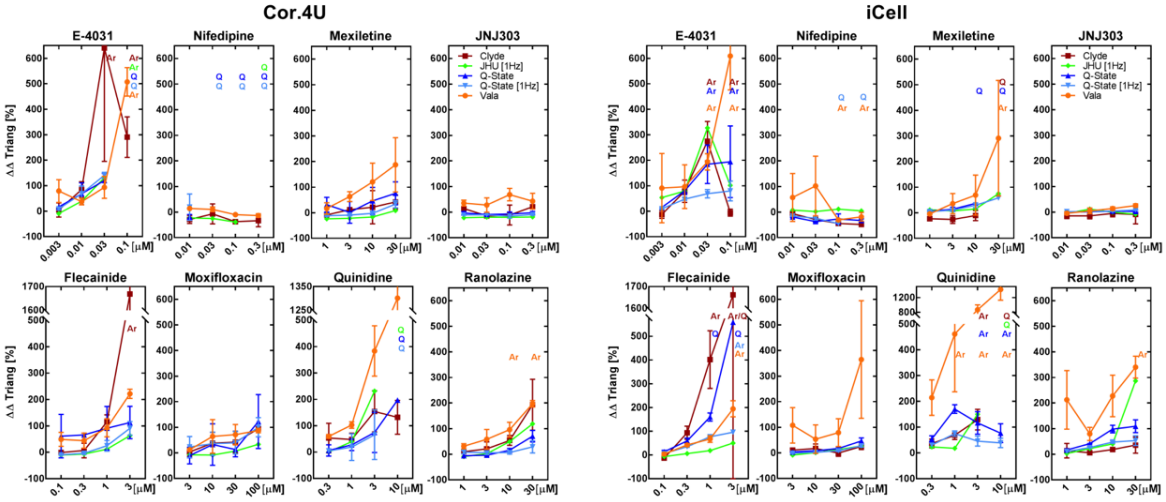

G Triang/APD$_{90}$

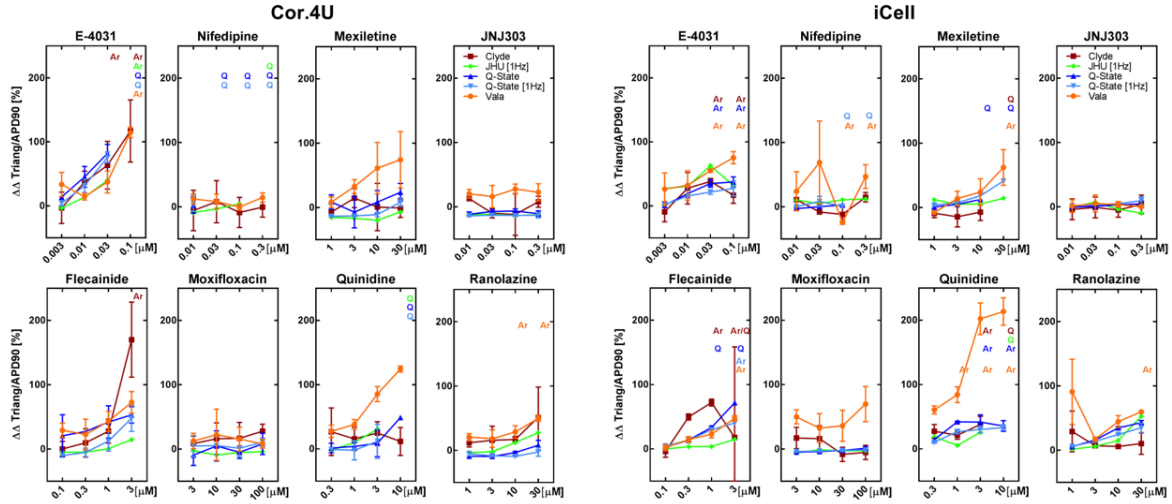

Supplemental Figure 2. Change in action potential parameters in response to all drugs from all four test sites. Plots of the mean and standard error of the relative change from vehicle control of: (A) (Spontaneous) Cycle length (CL), (B) APD$_{30}$, (C) APD$_{60}$, (D) APD$_{90}$, (E) Rise time (Trise), (F) Triangulation (Triang), and (G) Normalized triangulation (Triang/APD$_{90}$). (Left column) Cor.4U and (right column) iCell cardiomyocytes, under spontaneously beating (spont) or electrically or electrically/optically paced (1Hz) conditions. Q, Ar denote events described in **Table 5**.

Supplemental References

1. Aliot, E., Capucci, A., Crijns, H., Goette, A., & Tamargo, J. (2011). Twenty-five years in the making: flecainide is safe and effective for the management of atrial fibrillation. *Europace, 13*, 161-173.
2. Anderson, J. L., Lutz, J. R., & Allison, S. B. (1983). Electrophysiologic and antiarrhythmic effects of oral flecainide in patients with inducible ventricular tachycardia. *J Am Coll Cardiol, 2*, 105-114.
3. Antzelevitch, C., Belardinelli, L., Wu, L., Fraser, H., Zygmunt, A. C., Burashnikov, A., Di Diego, J. M., Fish, J. M., Cordeiro, J. M., Goodrow, R. J., Jr., Scornik, F., & Perez, G. (2004). Electrophysiologic properties and antiarrhythmic actions of a novel antianginal agent. *J Cardiovasc Pharmacol Ther, 9 Suppl 1*, S65-83.
4. Balfour, J. A., & Wiseman, L. R. (1999). Moxifloxacin. *Drugs, 57*, 363-374.
5. Bayer. (2011). AVELOX (moxifloxacin hydrochloride) Tablet, film-coated, Injection, solution for IV use (Label). In U. S. FDA (Ed.).
6. Benton, R. E., Sale, M., Flockhart, D. A., & Woosley, R. L. (2000). Greater quinidine-induced QTc interval prolongation in women. *Clin Pharmacol Ther, 67*, 413-418.
7. Crumb, W. J., Jr., Vicente, J., Johannesen, L., & Strauss, D. G. (2016). An evaluation of 30 clinical drugs against the comprehensive in vitro proarrhythmia assay (CiPA) proposed ion channel panel. *J Pharmacol Toxicol Methods, 81*, 251-262.
8. CVTherapeutics. (2008). Ranexa (ranolazine) extended-release tablets (Label). In U. S. FDA (Ed.).
9. Darpö, B. (2001). Spectrum of drugs prolonging QT interval and the incidence of torsades de pointes. *Eur Heart J Suppl, 3*, K70-K80.
10. Doki, K., Homma, M., Kuga, K., Aonuma, K., Sakai, S., Yamaguchi, I., & Kohda, Y. (2007). Gender-associated differences in pharmacokinetics and anti-arrhythmic effects of flecainide in Japanese patients with supraventricular tachyarrhythmia. *Eur J Clin Pharmacol, 63*, 951-957.
11. Donovan, B. T., Bakshi, T., Galbraith, S. E., Nixon, C. J., Payne, L. A., & Martens, S. F. (2011). Utility of frozen cell lines in medium throughput electrophysiology screening of hERG and NaV1.5 blockade. *J Pharmacol Toxicol Methods, 64*, 269-276.
12. Duff, H. J., Roden, D. M., Maffucci, R. J., Vesper, B. S., Conard, G. J., Higgins, S. B., Oates, J. A., Smith, R. F., & Woosley, R. L. (1981). Suppression of resistant ventricular arrhythmias by twice daily dosing with flecainide. *Am J Cardiol, 48*, 1133-1140.
13. Florian, J. A., Tornoe, C. W., Brundage, R., Parekh, A., & Garnett, C. E. (2011). Population pharmacokinetic and concentration--QTc models for moxifloxacin: pooled analysis of 20 thorough QT studies. *J Clin Pharmacol, 51*, 1152-1162.
14. Fossa, A. A., DePasquale, M. J., Raunig, D. L., Avery, M. J., & Leishman, D. J. (2002). The relationship of clinical QT prolongation to outcome in the conscious dog using a beat-to-beat QT-RR interval assessment. *J Pharmacol Exp Ther, 302*, 828-833.
15. Fujiki, A., Tani, M., Mizumaki, K., Shimono, M., & Inoue, H. (1994). Electrophysiologic effects of intravenous E-4031, a novel class III antiarrhythmic agent, in patients with supraventricular tachyarrhythmias. *J Cardiovasc Pharmacol, 23*, 374-378.
16. Garnett, C. E., Beasley, N., Bhattaram, V. A., Jadhav, P. R., Madabushi, R., Stockbridge, N., Tornoe, C. W., Wang, Y., Zhu, H., & Gobburu, J. V. (2008). Concentration-QT relationships play a key role in the evaluation of proarrhythmic risk during regulatory review. *J Clin Pharmacol, 48*, 13-18.

17. Gintant, G. (2011). An evaluation of hERG current assay performance: Translating preclinical safety studies to clinical QT prolongation. *Pharmacol Ther, 129*, 109-119.
18. Gualdani, R., Tadini-Buoninsegni, F., Roselli, M., Defrenza, I., Contino, M., Colabufo, N. A., & Lentini, G. (2015). Inhibition of hERG potassium channel by the antiarrhythmic agent mexiletine and its metabolite m-hydroxymexiletine. *Pharmacol Res Perspect, 3*, e00160.
19. Häselbart, V., Doevendans , J., & Wolf, M. (1981). Kinetics and bioavailability of mexiletine in healthy subjects. *Clin Pharmacol Ther, 29*.
20. Heath, B. M., Cui, Y., Worton, S., Lawton, B., Ward, G., Ballini, E., Doe, C. P., Ellis, C., Patel, B. A., & McMahon, N. C. (2011). Translation of flecainide- and mexiletine-induced cardiac sodium channel inhibition and ventricular conduction slowing from nonclinical models to clinical. *J Pharmacol Toxicol Methods, 63*, 258-268.
21. Jerling, M. (2006). Clinical pharmacokinetics of ranolazine. *Clin Pharmacokinet, 45*, 469-491.
22. Kleinbloesem, C. H., van Brummelen, P., van de Linde, J. A., Voogd, P. J., & Breimer, D. D. (1984). Nifedipine: kinetics and dynamics in healthy subjects. *Clin Pharmacol Ther, 35*, 742-749.
23. Kramer, J., Obejero-Paz, C. A., Myatt, G., Kuryshev, Y. A., Bruening-Wright, A., Verducci, J. S., & Brown, A. M. (2013). MICE models: superior to the HERG model in predicting Torsade de Pointes. *Sci Rep, 3*, 2100.
24. Li, Z., Dutta, S., Sheng, J., Tran, P. N., Wu, W., Chang, K., Mdluli, T., Strauss, D. G., & Colatsky, T. (2017). Improving the in silico assessment of proarrhythmia risk by combining hERG (human Ether-a-go-go-Related Gene) channel-drug binding kinetics and multichannel pharmacology. *Circ Arrhythm Electrophysiol, 10*, e004628.
25. Lombardo F, Obach RS, Shalaeva MY, & F, G. (2002). Prediction of volume of distribution values in humans for neutral and basic drugs using physicochemical measurements and plasma protein binding data. *J Med Chem, 45*, 2867-2876.
26. Lu, H. R., Vlaminckx, E., Van de Water, A., Rohrbacher, J., Hermans, A., & Gallacher, D. J. (2006). In-vitro experimental models for the risk assessment of antibiotic-induced QT prolongation. *Eur J Pharmacol, 553*, 229-239.
27. Min, D. I., Ku, Y. M., Geraets, D. R., & Lee, H. (1996). Effect of grapefruit juice on the pharmacokinetics and pharmacodynamics of quinidine in healthy volunteers. *J Clin Pharmacol, 36*, 469-476.
28. Noel, G. J., Natarajan, J., Chien, S., Hunt, T. L., Goodman, D. B., & Abels, R. (2003). Effects of three fluoroquinolones on QT interval in healthy adults after single doses. *Clin Pharmacol Ther, 73*, 292-303.
29. Olatunde, A., & Price Evans, D. A. (1982). Blood quinidine levels and cardiac effects in white British and Nigerian subjects. *Br J Clin Pharmacol, 14*, 513-518.
30. Omata, T., Kasai, C., Hashimoto, M., Hombo, T., & Yamamoto, K. (2005). QT PRODACT: comparison of non-clinical studies for drug-induced delay in ventricular repolarization and their role in safety evaluation in humans. *J Pharmacol Sci, 99*, 531-541.
31. Rajamani, S., Shryock, J. C., & Belardinelli, L. (2008). Rapid kinetic interactions of ranolazine with HERG K+ current. *J Cardiovasc Pharmacol, 51*, 581-589.
32. Redfern, W. S., Carlsson, L., Davis, A. S., Lynch, W. G., MacKenzie, I., Palethorpe, S., Siegl, P. K., Strang, I., Sullivan, A. T., Wallis, R., Camm, A. J., & Hammond, T. G. (2003). Relationships between preclinical cardiac electrophysiology, clinical QT interval prolongation and torsade de pointes for a broad range of drugs: evidence for a provisional safety margin in drug development. *Cardiovasc Res, 58*, 32-45.

33. Robertson, D. R., Waller, D. G., Renwick, A. G., & George, C. F. (1988). Age-related changes in the pharmacokinetics and pharmacodynamics of nifedipine. *Br J Clin Pharmacol, 25*, 297-305.
34. Schram, G., Zhang, L., Derakhchan, K., Ehrlich, J. R., Belardinelli, L., & Nattel, S. (2004). Ranolazine: ion-channel-blocking actions and in vivo electrophysiological effects. *Br J Pharmacol, 142*, 1300-1308.
35. Shah, R. (2013). Drug-induced QT interval prolongation: does ethnicity of the thorough QT study population matter? *Br J Clin Pharmacol, 75*, 347-358.
36. Shin, J.-G., Kang, W.-k., Shon, J.-H., Arefayene, M., Yoon, Y.-R., Kim, K.-A., Kim, D.-I., Kim, D.-S., Cho, K.-H., Woosley, R. L., & Flockhart, D. A. (2007). Possible interethnic differences in quinidine-induced QT prolongation between healthy Caucasian and Korean subjects. *Br J Clin Pharmacol, 63*, 206-215.
37. Stass, H., Dalhoff, A., Kubitza, D., & Schuhly, U. (1998). Pharmacokinetics, safety, and tolerability of ascending single doses of moxifloxacin, a new 8-methoxy quinolone, administered to healthy subjects. *Antimicrob Agents Chemother, 42*, 2060-2065.
38. Tan, Q. Y., Li, H. D., Zhu, R. H., Zhang, Q. Z., Zhang, J., & Peng, W. X. (2013). Tolerability and pharmacokinetics of ranolazine following single and multiple sustained-release doses in Chinese healthy adult volunteers: a randomized, open-label, Latin square design, phase I study. *Am J Cardiovasc Drugs, 13*, 17-25.
39. Towart, R., Linders, J. T., Hermans, A. N., Rohrbacher, J., van der Linde, H. J., Ercken, M., Cik, M., Roevens, P., Teisman, A., & Gallacher, D. J. (2009). Blockade of the I(Ks) potassium channel: an overlooked cardiovascular liability in drug safety screening? *J Pharmacol Toxicol Methods, 60*, 1-10.
40. Yamazaki, K., & Kanaoka, M. (2004). Computational prediction of the plasma protein-binding percent of diverse pharmaceutical compounds. *J Pharm Sci, 93*, 1480-1494.